Automatica 176 (2025) 112240

Contents lists available at ScienceDirect

Automatica

journal homepage: www.elsevier.com/locate/automatica

Optimal control over Markovian wireless communication channels under generalized packet dropout compensation ☆

Yuriy Zacchia Lun [a,*], Francesco Smarra [b], Alessandro D'Innocenzo [a]

[a] Department of Information Engineering, Computer Science and Mathematics, University of L'Aquila, 67100 L'Aquila, Italy
[b] Department of Civil, Construction-Architectural & Environmental Engineering, University of L'Aquila, 67100 L'Aquila, Italy

ARTICLE INFO

Article history:
Received 24 May 2024
Received in revised form 22 November 2024
Accepted 29 January 2025
Available online xxxx

Keywords:
Networked control systems
Wireless communications
Telecommunication-based automation systems

ABSTRACT

Control loops closed over wireless links greatly benefit from accurate estimates of the communication channel condition. To this end, the finite-state Markov channel model allows for reliable channel state estimation. This paper develops a Markov jump linear system representation for wireless networked control with persistent channel state observation, stochastic message losses, and generalized packet dropout compensation. With this model, we solve the finite- and infinite-horizon linear quadratic regulation problems and introduce an easy-to-test stability condition for any given infinite-horizon control law. We also thoroughly analyze the impact of a scalar general dropout compensation factor on the stability and closed-loop performance of a rotary inverted pendulum controlled remotely through a wireless link. Finally, we validate the results numerically via extensive Monte Carlo simulations, showing the benefits of the proposed control strategy.

1. Introduction

Wireless networked control systems receive considerable attention from industry and academia thanks to their mission-critical applications in industrial automation, intelligent transportation, telesurgery, and smart grids. See, e.g., Park, Ergen, Fischione, Lu, and Johansson (2018), Eisen, Rashid, Gatsis, Cavalcanti, Himayat, and Ribeiro (2019), Pezzutto, Tramarin, Dey, and Schenato (2020), and Liu, Nair, Li, Nesic, Vucetic, and Poor (2021) as an overview of significant recent advances in the wireless networked control system research. One of the central topics in this research area is estimation and control over fading channels, explored, e.g., in Schenato, Sinopoli, Franceschetti, Poolla, and Sastry (2007), Gupta, Dana, Hespanha, Murray, and Hassibi (2009), Heemels, Teel, van de Wouw, and Nesic (2010), Gonçalves, Fioravanti, and Geromel (2010), Ding (2011), Pajic, Sundaram, Pappas, and Mangharam (2011), Minero, Coviello, and Franceschetti (2013), Quevedo, Østergaard, and Ahlén (2014), Yu and Fu (2015), Zacchia Lun and D'Innocenzo (2019), Liu, Quevedo, Li, Johansson, and Vucetic (2022), Impicciatore, Tsiamis, Zacchia Lun, D'Innocenzo, and Pappas (2022), and Impicciatore, Zacchia Lun, Pepe, and D'Innocenzo (2024).

The performance of systems having their control loops closed over wireless links is strongly affected by the communication channels' stochastic behavior since wireless links are subject to path loss, shadowing, and fading when mobility is involved: this gives rise to time-varying message dropouts, message delays, and jitter (Goldsmith, 2005). Consequently, an accurate estimate of the channel condition for correctly modeling the stochastic properties of a wireless networked control system can significantly increase the control performance.

The finite-state Markov channel (FSMC; see, e.g., Sadeghi, Kennedy, Rapajic, & Shams, 2008) is a simple yet powerful analytical model that captures the dynamics of the wireless link. It is widely used for analyzing and designing telecommunications systems. Despite the availability of the FSMC model, when dealing with the application level, packet dropouts dynamics are often modeled as realizations of a Bernoulli process (Hu, Shi, Zhang, & Deng, 2021; Schenato et al., 2007), which may result in an oversimplification of the complex communication subsystem dynamics and, thus, in an incorrect analysis of the control subsystem properties, for instance in terms of stability (Zacchia Lun & D'Innocenzo, 2019).

1.1. Study motivation and technical challenges

Recently, Impicciatore et al. (2024) introduced FSMC models into a wireless networked control framework for optimal output-feedback control, proving the validity of the separation principle, which allows for designing the optimal remote system state estimator and controller separately. It showed that due

☆ The material in this paper was not presented at any conference. This paper was recommended for publication in revised form by Associate Editor Luca Schenato under the direction of Editor Christos G. Cassandras.

* Corresponding author.
E-mail addresses: yuriy.zacchialun@univaq.it (Y. Zacchia Lun), francesco.smarra@univaq.it (F. Smarra), alessandro.dinnocenzo@univaq.it (A. D'Innocenzo).

https://doi.org/10.1016/j.automatica.2025.112240

to the one-time-step delayed channel state observation by the remote controller, the optimal control over FSMC links problem represents the main challenge in wireless output-feedback control since for the same FSMC link characteristics, the remote system may be detectable but not controllable. One significant limitation of Impicciatore et al. (2024) addressed in this paper is considering only the zero-input packet dropout compensation at the actuator end, which results in sub-optimal performance. To fill this gap, this paper exploits an FSMC wireless link abstraction to model packet dropouts, as in Zacchia Lun, Rinaldi, Alrish, D'Innocenzo, and Santucci (2020). Similarly to Impicciatore et al. (2024) and Zacchia Lun, Rinaldi, D'Innocenzo, and Santucci (2024), it considers a persistent channel state observation, providing a controller with the outcome of each control packet transmission and observed state channel state in a positive or negative acknowledgment message. However, this paper introduces a generalized control packet dropout compensator to the closed-loop system architecture. Specifically, the actuators apply an appropriately scaled last available control input when the communication link corrupts a transmitted control message. This approach encompasses both zero-input and hold-input packet dropout compensations as notable cases, and it is particularly suitable for less performant actuators incapable of immediately zeroing the control inputs. Markedly, this article differs from previous works on generalized control packet dropout compensation, such as Moayedi, Foo, and Soh (2013), Yu and Fu (2015), and Lu, Zhong, and Qu (2018), in considering the FSMC to govern the packet dropout dynamics instead of the Bernoulli process, resulting in a much more general and complex problem setup presented in Section 2. The generalized control packet dropout compensation strategy is straightforward, intuitive, and structurally simple, making it appealing from the implementation and cost perspectives (Yu & Fu, 2015). Other compensators can, in principle, be constructed based on a static or dynamic, linear or nonlinear combination of several past controls at different previous time instants. Still, such compensators would be more costly, complex, and energy-consuming.

Considering the generalized control packet dropout compensation within the wireless networked control framework under the FSMC link model presents several major technical challenges and offers a significant increase in control performance, as demonstrated in Sections 7.6 and 7.7. The first challenge lies within the controller specification and the resulting closed-loop system model. It requires answering whether the control gain should depend only on the last observed channel state or whether some additional information, such as the current packet dropout interval, is necessary. This paper shows in Section 3.2 that the channel state information is sufficient for selecting the optimal control gain at run time, thus limiting the complexity and the related processing delay. However, the closed-loop system model must consider the FSMC-state-dependent packet dropout interval process, requiring different novel perspectives for control design and stability analysis, as detailed in Sections 3.2 and 5.1. An additional challenge of the finite-horizon optimal controller design also comes from the stochastic nature of the packet dropout interval, which requires the controller to balance the time horizon and the possible number of consecutive control message dropouts at each time step, as detailed in Section 4. For the infinite-horizon case, establishing the ergodicity of the closed-loop system's discrete dynamics is another significant technical challenge addressed in this paper in Proposition 15. None of these challenges were tackled in the current wireless networked control system literature. Only successfully addressing them allows us to cast and solve optimally the discrete-time linear stochastic systems with information between sensors, controllers, and actuators carried by FSMCs in a Markovian jump linear system (MJLS) framework and to rely on its fundamental principles.

1.2. Related works

The MJLS theory has been extensively used to investigate feedback control problems over lossy links.

Several works used a simplified Gilbert channel modeled by a Markov chain with two states. Specifically, Seiler and Sengupta (2005) derived necessary and sufficient linear matrix inequality (LMI) conditions for synthesizing the optimal H_∞ controller, assuming the controller is collocated with the actuator so that only the sensor measurements may be lost. Kawka and Alleyne (2006) analyzed the stability and performance of a channel-state-independent (CSI) controller with N-step packet loss compensation under one step of actuation delay, where transmitting packets containing multiple control inputs increases actuation delay and packet error probability due to larger packet size. Xie and Xie (2009) investigated stability properties of sampled-data networked linear systems under CSI control. You and Xie (2010) derived the minimum data rate for mean square (MS) stabilizability under an arbitrary CSI quantized state-feedback (SF) control policy. Minero et al. (2013) extended this result to a time-varying data rate modeled by a finite-state Markov chain. Mo, Garone, and Sinopoli (2013) solved finite- and infinite-horizon CSI linear–quadratic–Gaussian (LQG) control problems and proved the validity of the separation principle. Battilotti, Cacace, d'Angelo, Germani, and Sinopoli (2019) extended the finite-horizon CSI result to a non-Gaussian setting, assuming that the moments of the noise sequences up to the fourth order are known. Okano and Ishii (2017) derived conditions for MS stability of uncertain autoregressive systems whose state and input parameters vary within given intervals and characterized limitations on data rate, packet loss probabilities, and magnitudes of parametric uncertainty under CSI control. Finally, Li, Han, Zhang, Xie (2021) and Li, Li, Zhang (2021) solved the finite- and infinite-horizon linear–quadratic regulation (LQR) problems for discrete-time systems with a known constant input delay for the zero-input and hold-input control packet dropout compensation, respectively. However, the two-state Markov chain model used in all the works above cannot represent a nontrivial FSMC (Impicciatore et al., 2024). Moreover, disregarding the Markov channel state in the control design leads to simpler but more conservative solutions that apply only to a subset of plants stabilizable with channel-state-dependent controllers (Impicciatore et al., 2024).

Some works used a finite-state Markov chain to describe the evolution of a packet error burst length without considering the observed communication channel state. In particular, Wu and Chen (2007) derived sufficient LMI conditions and corresponding control laws for the stochastic stability of noiseless systems with hold-input packet dropout compensation at the controller and actuator end. Wang, Wang, and Wang (2013) presented an H_∞ SF control method and sufficient conditions for controllers ensuring stochastic stability with a specific disturbance attenuation level. Other works relied on a finite-state Markov chain description of all possible packet arrival sequences of a certain length. These models also did not consider the Markov channel state information. A notable example is Peters, Marelli, Quevedo, and Fu (2019), which addressed the predictive control design problem for networked systems subject to packet loss in the controller-to-actuator link. Additional noteworthy works characterized the packet losses in combination with other significant concerns, such as jamming attacks on communication links (Cetinkaya, Ishii, & Hayakawa, 2017) and random delays (Xu, Gu, Tang, & Qian, 2022). Still, the Markov channel state information was neglected.

1.3. Contribution statement

The main contributions of this paper are the following.

(1) We present a practical Markov jump linear system model of discrete-time linear stochastic systems with a generalized control message dropout compensation over lossy actuation links modeled by FSMCs (see Section 3).
(2) We solve finite- and infinite-horizon LQR problems, providing the SF gains that depend on the FSMC state observed with one time-step delay (Sections 4 and 6 and Remark 7).
(3) We introduce a necessary and sufficient stability condition for any given infinite-horizon SF control law that requires computing the spectral radius of a stability verification matrix and, thus, is easy to check (see Section 5).
(4) We validate all theoretical results numerically via extensive Monte Carlo simulations of a rotary inverted pendulum controlled remotely over a wireless link, where the link model relies on an accurate representation of a realistic wireless communication protocol. Furthermore, we provide a comparative analysis of proposed and existing LQR strategies and illustrate the impact of a scalar general dropout compensation factor on stability and closed-loop performance (see Section 7).

2. Model and problem formulation

Consider a discrete-time linear stochastic system with intermittent control messages due to lossy communication and generalized dropout compensation:

$$\begin{cases} x_{k+1} = Ax_k + Bu_k + w_k, \\ u_k = \delta_k u_k^c + (1-\delta_k)\Phi u_{k-1}. \end{cases} \tag{1}$$

We use a standard notation, where $x_k \in \mathbb{R}^{n_x}$ and $u_k \in \mathbb{R}^{n_u}$ are a system state and a control input to actuators, while A and B are state and input matrices of appropriate size, respectively; $w_k \in \mathbb{R}^{n_x}$ is a white Gaussian process noise having zero mean and covariance matrix Σ_w.

Assumption 1. The process noise w_k is independent of the initial state x_0 and the binary stochastic variable δ_k.

In the expression of u_k, δ_k models the packet loss between the controller and the actuators, and $u_k^c \in \mathbb{R}^{n_u}$ is the desired control input computed by the remote controller. If the control message is correctly delivered, $u_k = u_k^c$; otherwise, if lost, the actuators apply the last available control input multiplied by a matrix $\Phi = \bigoplus_{i=1}^{n_u} \phi_i$, where $\oplus$ indicates the direct sum that produces a diagonal matrix with the elements $\phi_i \in [0, 1]$ on the main diagonal. This generalized approach covers both the zero-input (with all $\phi_i = 0$) and hold-input (with all $\phi_i = 1$) control message dropout compensations as its particular cases.

We capture the dynamics of the control packet loss process $\{\delta_k\}$ in wireless links via an FSMC (Sadeghi et al., 2008) abstraction.[1] The wireless channel state is the output of a discrete-time Markov chain (DTMC) taking values in a finite set $\mathcal{S} \triangleq \{s_i\}_{i=1}^N$. This state conditions the probability of successful packet delivery and packet loss:

$$\begin{aligned} &\mathbb{P}(\delta_k = 1 \mid \theta_k = s_i) = \hat{\delta}_i, \\ &\mathbb{P}(\delta_k = 0 \mid \theta_k = s_i) = 1 - \hat{\delta}_i. \end{aligned} \tag{2}$$

[1] See, e.g., Zacchia Lun et al. (2020) for a procedure producing a consistent and accurate FSMC model suitable for a wireless industrial automation scenario.

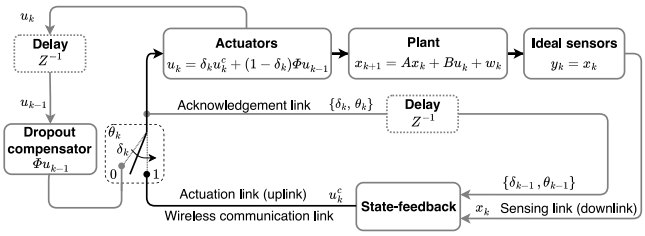

Fig. 1. Closed-loop system architecture. A wireless link delivers SF control inputs to actuators. The receiver measures the link state θ_k and communicates it with the transmission outcome δ_k to the controller. The actuators apply the generalized packet dropout compensation.

In other words, we relate each state s_i of the FSMC to a binary symmetric channel with error probability $1-\hat{\delta}_i$. The probabilities of transitions between FSMC states

$$p_{ij} \triangleq \mathbb{P}(\theta_k = s_j \mid \theta_{k-1} = s_i) \geq 0, \quad \sum_{j=1}^{N} p_{ij} = 1. \tag{3}$$

We gather them into the channel transition probability matrix (TPM)

$$P_c \triangleq \left[p_{ij}\right]_{i,j=1}^{N}. \tag{4}$$

Assumption 2. The DTMC $\{\theta_k\}$ is ergodic.

Assumption 3. The process noise $\{w_k\}$ and the DTMC $\{\theta_k\}$ are independent.

In many practical wireless communication scenarios, for instance, when networks rely on IEEE 802.15.4-compatible hardware,[2] the FSMC state is available to receivers (Zacchia Lun et al., 2020). So, as in Zacchia Lun and D'Innocenzo (2019), we assume that a controller may observe Markov channel states via positive and negative acknowledgments (ACKs and N-ACKs), which become available only after the current decision on the control gain to apply has been made and sent through the wireless link since the actual transmission outcome is unknown in advance. Formally, the information set available to the controller is

$$\mathcal{I}_k = \left\{(x_t)_{t=0}^k, (\delta_{t-1})_{t=1}^k, (\theta_{t-1})_{t=1}^k\right\}. \tag{5}$$

It relies on an idealistic assumption of accessing all system state variables over an error free link made only to streamline the presentation. We have already shown in Impicciatore et al. (2024) how to design the optimal output-feedback controller by solving the optimal SF control and optimal filtering problems separately for a networked control scenario with the zero-input compensation strategy for the packet losses in the wireless links conveying sensing and actuation data. Since the acknowledgment messages transporting the related transmission outcome and channel state information are short and unlikely to be corrupted, we also make an idealistic assumption that all the ACKs are always successfully delivered.[3] Fig. 1 shows the closed-loop system architecture, and Fig. 2 provides the related timing diagram. This paper solves the following design problem.

Problem statement: Design a finite- or infinite-horizon controller for the system (1) that fully exploits its information set

[2] The typical networking protocols for wireless industrial automation, such as WirelessHART, ISA100.11a, and Zigbee PRO 2015, use IEEE 802.15.4.

[3] One can readily relax it by introducing an additional binary stochastic variable to model the successful delivery of the ACK that would evolve according to an FSMC describing the corresponding wireless link.

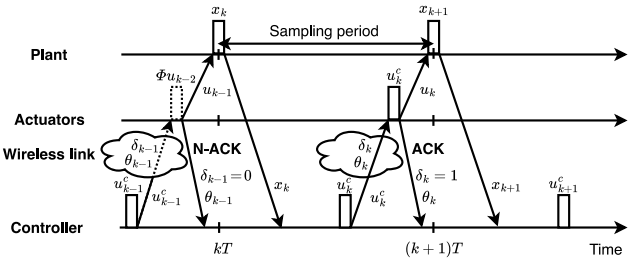

Fig. 2. A timing diagram for a closed-loop system with a wireless actuation link. In this example, the transmission corrupts the control packet containing u^c_{k-1}, as indicated by a dotted line. The receiver detects an error, discards the message, and sends the N-ACK containing the channel state θ_{k-1}. Actuators compensate by applying a scaled version of the previous input signal, i.e. $u_{k-1} = \Phi u_{k-2}$ depicted by a dotted rectangular. The solid line in a cloud indicates successful wireless transmission of the control message u^c_k to be applied by actuators so that $u_k = u^c_k$. Thus, the receiver sends the ACK also containing the channel state, i.e., θ_k.

(5). Thus, the SF gain should depend on the Markov channel state observed with one time-step delay[4]:

$$u^c_k = K_{(k,\theta_{k-1})} x_k. \tag{6}$$

Specifically, consider a time horizon $T \in \mathbb{Z}^{>} \cup \{\infty\}$ and denote by $\mathcal{U}_T$ a set of all control inputs satisfying (6). In the following, $\mathbb{Z}^{>}$ and $\mathbb{Z}^{\geq}$ will indicate the sets of all positive and nonnegative integers, respectively. Given a positive semi-definite state-weighting matrix $Q \in \mathbb{R}^{n_x}$ and a positive-definite input-weighting matrix $R \in \mathbb{R}^{n_u}$, the optimal linear quadratic regulator minimizes the following costs. Denote by $\mathbb{E}$ the expectation. For $T < \infty$,

$$J_T(x_0, \mathcal{U}_T) = \mathbb{E}\left(\sum_{k=0}^{T-1} \left(x_k^\top Q x_k + u_k^\top R u_k \right) + x_T^\top Q x_T \mid \mathcal{I}_0 \right), \tag{7}$$

where $^\top$ indicates the transpose. Notice that the cost (7) weights the inputs to actuators and, thus, accounts for both the dropout compensation gain Φ and the desired control inputs $u^c_k \in \mathcal{U}_T$, depending on the realizations of the stochastic process $\{\delta_k\}$. So, the following optimization problem defines the finite-horizon LQR paradigm:

$$\check{\mathbf{u}}^c_T = \underset{\mathbf{u}^c_T \in \mathcal{U}_T}{\arg\min} J_T(x_0, \mathcal{U}_T), \tag{8}$$

where $\mathbf{u}^c_T \triangleq \left(u^c_t\right)_{t=0}^{T-1}$ is a sequence of control inputs. For $T = \infty$, consider the long-run average cost

$$J_\infty(x_0, \mathcal{U}_\infty) = \limsup_{T\to\infty} \frac{1}{T} J_T(x_0, \mathcal{U}_T). \tag{9}$$

Then, the solution of the following optimization problem defines the infinite-horizon LQR paradigm:

$$\check{\mathbf{u}}^c_\infty = \underset{\mathbf{u}^c_\infty \in \mathcal{U}_\infty}{\arg\min} J_\infty(x_0, \mathcal{U}_\infty). \tag{10}$$

To analytically solve problems (8) and (10) in the FSMC setting, we first represent system (1) in the Markovian jump linear system (MJLS) framework, as detailed next.

[4] See Remark 6 for the technical motivation for the control gain dependence on the channel state but not the observed values of the packet loss process. Intuitively, the system state x_k contains the transmission outcome information encoded in $(\delta_{t-1})_{t=1}^k$.

3. Markovian jump system model for control

This section derives an MJLS model that accounts for a generalized control message dropout compensation over a lossy actuation link modeled as an FSMC. After characterizing the system states in opportune time instances in Section 3.1, it defines the system's discrete states and the related transition probabilities for the LQR in Section 3.2.

3.1. System states in packet delivery time instances

The intuition behind the MJLS derivation is that system (1) has a unique and convenient representation in the time instances in which actuators successfully receive messages from controllers. These time instances differ by a nonnegative number of consecutive control message dropouts governed by an FSMC. Thus, we count the number of consecutive control message dropouts observable by a controller at a given time step k in a stochastic variable Δ_k. The value of Δ_k increments by one when the reception of a control message is not acknowledged and resets to zero otherwise. Formally,

$$\Delta_k = (1 - \delta_{k-1})(\Delta_{k-1} + 1). \tag{11}$$

By iterating (11) over multiple time steps, we have that

$$\Delta_k = \ell \Leftrightarrow \delta_{k-1-\ell} = 1 \wedge \delta_{k-t} = 0 \ \forall t \in \mathbb{Z}^{>} : t \leq \ell. \tag{12}$$

Notice that if $\ell = 0$, then $\{t\}_{t=1}^0 = \emptyset$, meaning that (12) becomes $\Delta_k = 0 \Leftrightarrow \delta_{k-1} = 1$.

Let $\mathcal{T}$ be a set of time instances in which actuators successfully receive the controller's messages, i.e.,

$$\mathcal{T} \triangleq \{k : \delta_k = 1\}_{k\in\mathbb{Z}^{\geq}} = \left\{\tau_{(m)}\right\}_{m\in\mathbb{Z}^{\geq}}. \tag{13a}$$

From (11), (12), and (13a), for all $m \in \mathbb{Z}^{\geq}$,

$$\tau_{(m)} \in \mathcal{T} \Rightarrow \delta_{\tau_{(m)}} = 1 \Rightarrow \Delta_{\tau_{(m)}+1} = 0, \tag{13b}$$

$$\tau_{(m+1)} = \tau_{(m)} + 1 + \Delta_{\tau_{(m+1)}}. \tag{13c}$$

For notational convenience, for any $k, n \in \mathbb{Z}^{\geq}$, let

$$\Psi_{(n)} \triangleq \sum_{j=0}^{n} A^j B \Phi^{n-j}, \tag{14}$$

$$\Gamma_{(k,n)} \triangleq \sum_{j=0}^{n} A^{n-j} w_{k+j}. \tag{15}$$

Then, the following proposition provides the foundation for the technical results of the paper.

Proposition 4. *The system (1) with control packet loss process $\{\delta_k\}$ governed by an FSMC described by (2)–(4) and an arbitrary control strategy satisfying (6) is trace-equivalent to the following system, where the components and time instances are defined by (11)–(15).*

$$\begin{cases} \Delta_{\tau_{(m+1)}} = n \in \mathbb{Z}^{\geq} \Rightarrow \forall h \in \mathbb{Z}^{\geq} : h \leq n, \\ x_{\tau_{(m)}+1+h} = A^{h+1} x_{\tau_{(m)}} + \Psi_{(h)} u_{\tau_{(m)}} + \Gamma_{(\tau_{(m)},h)}, \\ u_{\tau_{(m)}+h} = \Phi^h K_{(\tau_{(m)},\theta_{\tau_{(m)}-1})} x_{\tau_{(m)}}. \end{cases} \tag{16}$$

Proof. By construction, (11)–(16) describe the dynamics of the system (1)–(4) constrained by (6).

Remark 5. Proposition 4 does not address transition probabilities between $\tau_{(m)}$ and $\tau_{(m+1)}$, and the trace equivalence means that for any given initial system state x_0, control law satisfying (6), and realization of $(\delta_t)_{t=0}^{\tau_m+n}$ and $(w_t)_{t=0}^{\tau_m+n}$, the states $x_{\tau_{(m)}}$ and $x_{\tau_{(m)}+1+h}$

obtained from (1) and (16) will be the same $\forall h \in \mathbb{Z}^{\geq}$ such that $h \leq n$. Taken alone, (16) presents all possible effects of packet error bursts and a control command satisfying (6) under the generalized packet dropout compensation on the system state dynamics when considered for arbitrary values $n \in \mathbb{Z}^{\geq}$ of $\Delta_{\tau_{(m+1)}}$ in the controller's perspective. On the contrary, for any observed sequence of time instances in $\mathcal{T}$, (16) reproduces the dynamics of (1) in these time instances from the actuators' and plant's perspective. Notice from (13) that time instances in $\mathcal{T}$ must obey (2)–(3).

System (16) formalizes that all the system states that precede a state with successful reception of a controller's message depend on the previously received control command, the duration of a packet error burst following the last successful control message reception, the packet dropout compensation strategy, and the evolution of the process noise. Besides, (5), (11), and (13) make clear that the number of consecutive control message dropouts following a successful reception of a control command is unknown to a controller beforehand. However, the current number of consecutive control message dropouts $\Delta_{\tau_{(m)}}$ and the previous FSMC state $\theta_{\tau_{(m)}-1}$ are part of the controller's information set $\mathcal{I}_{\tau_{(m)}}$. To find the expression of the control gain, define the operational modes of a system (16) from the controller's perspective as follows.

3.2. System model for the LQR

Group together the current duration of a packet error burst and the last known wireless channel state in one augmented discrete state: $\eta_k \triangleq (\Delta_k, \theta_{k-1})$. From (13),

$$\eta_{\tau_{(m)}} = (\Delta_{\tau_{(m)}}, \theta_{\tau_{(m)}-1}), \tag{17a}$$

$$\eta_{\tau_{(m+1)}} = (\Delta_{\tau_{(m+1)}}, \theta_{\tau_{(m)}+\Delta_{\tau_{(m+1)}}}), \tag{17b}$$

where $\Delta_{\tau_{(m+1)}}$ indicates the time interval the transmitted control input may remain active. From the controller's perspective, $\eta_{\tau_{(m)}}$ is known, while $\eta_{\tau_{(m+1)}}$ is a random variable. In what follows, we derive the conditional probability of $\eta_{\tau_{(m+1)}}$ with respect to $\eta_{\tau_{(m)}}$.

Denote by e_i the column vector of the standard basis of $\mathbb{R}^N$: all its components are zero except the ith, which equals one. Furthermore, store the probability of successful control packet delivery (or, conversely, of packet dropout) in a state of FSMC starting from a particular previous state in the matrix P_1 (or, respectively, P_0):

$$P_1 \triangleq [p_{ij}\hat{\delta}_j]_{i,j=1}^N, \; P_0 \triangleq [p_{ij}(1-\hat{\delta}_j)]_{i,j=1}^N = P_c - P_1. \tag{18}$$

Then, from (2)–(4), (11)–(13), (17), and (18), the chain rule of the probability and independence of both δ_k and θ_k of δ_{k-t} for all $t \in \mathbb{Z}^{>}$,

$$\begin{aligned}&\mathbb{P}(\eta_{\tau_{(m+1)}} = (n, s_j) \mid \eta_{\tau_{(m)}} = (\ell, s_i)) = \\ &\mathbb{P}(\delta_{\tau_{(m)}+t} = 0 \; \forall t \in \mathbb{Z}^{>} : t \leq n, \delta_{\tau_{(m)}+n+1} = 1, \theta_{\tau_{(m)}+n} = s_j \\ &\mid \theta_{\tau_{(m)}-1} = s_i, \delta_{\tau_{(m)}} = 1) = \frac{e_i^\top P_1 P_0^n e_j e_j^\top P_1 \mathbf{1}}{e_i^\top P_1 \mathbf{1}} \triangleq \zeta_{(i,n,j)}.\end{aligned} \tag{19}$$

In (19), $\mathbf{1}$ indicates the column vector of appropriate size with all components equal to one.

Remark 6. The transition probabilities in (19) are independent of $\Delta_{\tau_{(m)}}$. Thus, all augmented-discrete-state-dependent control gains with the same last known FSMC state $\theta_{\tau_{(m)}-1}$ have identical probabilities of being received successfully and remaining active during a packet error burst. Hence, the optimal mode-dependent control gains should be the same for any given value of $\theta_{\tau_{(m)}-1}$ regardless of the current duration of a packet error burst[5]: designing an optimal mode-dependent controller would produce an optimal FSMC-state-dependent controller, and substituting $\theta_{\tau_{(m)}-1}$ with $\eta_{\tau_{(m)}}$ in (16) would not alter the system's behavior under an optimal control law.

For the notational convenience, let

$$q_{in} \triangleq \sum_{j=1}^{N} \zeta_{(i,n,j)}, \quad \varsigma_{(n,j)} \triangleq P_0^n e_j e_j^\top P_1 \mathbf{1}, \tag{20a}$$

i.e., the vector of probabilities of an n-length packet error burst that ends with the FSMC being in state s_j, and

$$\zeta_{(i,n,j)} = \frac{e_i^\top P_1 \varsigma_{(n,j)}}{e_i^\top P_1 \mathbf{1}}, \tag{20b}$$

a compact form of the transition probability (19).

Notice from (2)–(4) and (18) that all the parameters in (20) are nonnegative and $\sum_{n\in\mathbb{Z}^{\geq}} \sum_{j=1}^{N} \varsigma_{(n,j)} = \mathbf{1}$. For big enough values $\hat{n}$ of a packet error burst $\Delta_{\tau_{(m+1)}}$, the probability $\varsigma_{(\hat{n},j)}$ becomes negligible and does not contribute to the summation above, i.e., there is a maximal number of consecutive control message dropouts $L \in \mathbb{Z}^{>}$ such that $\sum_{n=0}^{L} \sum_{j=1}^{N} \varsigma_{(n,j)} \geq (1-\epsilon)\mathbf{1}$, where ϵ is arbitrarily small. In the numerical case studies using floating-point arithmetic, ϵ typically corresponds to the machine epsilon. Thus, the maximal number of consecutive control message dropouts, L, results from the following optimization:

$$L \triangleq \arg\min_{\hat{n}\in\mathbb{Z}^{>}} \sum_{n=0}^{\hat{n}} \sum_{j=1}^{N} \varsigma_{(n,j)} \geq (1-\epsilon)\mathbf{1}, \tag{21}$$

easily solvable by, e.g., the bisection method.

Remark 7. The system matrices from the MJLS model (16), (17), and (19)–(21) depend on the future, not present, operational mode $\eta_{\tau_{(m+1)}}$ forecast by the controller based on transition probabilities (20b). Thus, the optimal mode-dependent SF control problem differs from the existing formulations presented, e.g., in Costa, Fragoso, and Marques (2005) and Matei, Martins, and Baras (2008) and provides a different, more complex solution averaging the effect of the control action through all possible packet error bursts.

Lemma 8. *The system (1)–(3) constrained by (5) and (6) is a MJLS described by (11)–(20).*

Proof. It follows from Proposition 4 and Remark 6.

4. Optimal finite-horizon LQR

This section provides the finite-horizon solution to the problem (8), one of the main contributions of this paper. In the finite-horizon setting, the control commands must balance the time horizon and possible number of consecutive control message dropouts at each time step. Specifically, on the one hand, a transmitted control command may remain active for a long time, up to the maximal number of consecutive control message dropouts L defined by (21). Thus, the control command should average its effects over the $L+1$ discrete states of the system. On the other hand, near the time horizon end, the most recent control commands may never reach the actuators if the number of consecutive control message dropouts becomes greater than

[5] Otherwise, applying different control gains would produce the same cost, and the solution to the optimization problem would not be unique, which is not the case in our setting.

the remaining time horizon. Thus, at the end of the time horizon, the control commands average the effects over fewer states. The following theorem formalizes this concept.

Theorem 9. *The finite-horizon LQR solving the problem (8) for the system (1)–(3) is given by*

$$\check{u}_k^c = K_{(k,\theta_{k-1})} x_k, \tag{22}$$

where, $\forall k \in \mathbb{Z}^{\geq} : k < T$ *and any value* $s_i \in \mathcal{S}$ *of* θ_{k-1},

$$K_{(k,s_i)} = -\mathcal{B}_{(k,s_i)}^{-1} \mathcal{C}_{(k,s_i)}, \tag{23}$$

$$\mathcal{C}_{(k,s_i)} = \sum_{h=0}^{L-\xi_k} q_{ih} \sum_{r=1}^{h} \Psi_{(r-1)}^{\top} Q A^r + \sum_{h=0}^{L-\xi_k} \sum_{j=1}^{N} \zeta_{(i,h,j)} \Psi_{(h)}^{\top} \mathcal{X}_{(k+1+h,s_j)} A^{h+1}, \tag{24a}$$

$$\mathcal{B}_{(k,s_i)} = R + \sum_{h=0}^{L-\xi_k} q_{ih} \sum_{r=1}^{h} \Phi^{r\top} R \Phi^r + \sum_{h=0}^{L-\xi_k} q_{ih} \sum_{r=1}^{h} \Psi_{(r-1)}^{\top} Q \Psi_{(r-1)} + \sum_{h=0}^{L-\xi_k} \sum_{j=1}^{N} \zeta_{(i,h,j)} \Psi_{(h)}^{\top} \mathcal{X}_{(k+1+h,s_j)} \Psi_{(h)}, \tag{24b}$$

$$\mathcal{X}_{(k,s_i)} = \mathcal{A}_{(k,s_i)} - \mathcal{C}_{(k,s_i)}^{\top} \mathcal{B}_{(k,s_i)}^{-1} \mathcal{C}_{(k,s_i)}, \tag{24c}$$

$$\mathcal{X}_{(T,s_i)} = Q, \tag{24d}$$

$$\mathcal{A}_{(k,s_i)} = Q + \sum_{h=0}^{L-\xi_k} q_{ih} \sum_{r=1}^{h} A^{r\top} Q A^r + \sum_{h=0}^{L-\xi_k} \sum_{j=1}^{N} \zeta_{(i,h,j)} (A^{h+1})^{\top} \mathcal{X}_{(k+1+h,s_j)} A^{h+1}, \tag{24e}$$

$$\xi_k \triangleq \max\{0, k+1+L-T\} \tag{24f}$$

so that $\xi_{T-1} = L$, *and* $\xi_k = 0$ *for all* $k < T - L$.

The optimal cost is

$$J_T^{\star}(x_0) = x_0^{\top} \left(\sum_{i=1}^{N} \vartheta_i \mathcal{X}_{(0,s_i)} \right) x_0 + \sum_{i=1}^{N} \vartheta_i g_{(0,s_i)}, \tag{25}$$

where $\{\vartheta_i\}$ *indicates the initial probability distribution of the FSMC's states, and, by convention,* $\theta_{-1} = \theta_0$, *so that*

$$\vartheta_i \triangleq \mathbb{E}\left(1_{\{\theta_0 = s_i\}}\right) = \mathbb{E}\left(1_{\{\theta_{-1} = s_i\}}\right), \tag{26}$$

$$g_{(k,s_i)} = \sum_{h=0}^{L-\xi_k} \sum_{j=1}^{N} e_i^{\top} \varsigma_{(h,j)} \left(\sum_{r=1}^{h} \sum_{\nu=0}^{r-1} \operatorname{tr}(A^{\nu\top} Q A^{\nu} \Sigma_W) + \sum_{\nu=0}^{h} \operatorname{tr}(A^{\nu\top} \mathcal{X}_{(k+1+h,s_j)} A^{\nu} \Sigma_W) + g_{(k+1+h,s_j)} \right), \quad g_{(T,s_i)} = 0. \tag{27}$$

Proof. See the Appendix.

5. Closed-loop system stability analysis

An infinite-horizon control strategy aims at guaranteeing the convergence of the system's state to an equilibrium point. This goal is achievable only for the stabilizable systems, formally defined as follows.

Definition 10 (*Stabilizability*)**.** A system (1)–(3) is stabilizable with one time-step delayed actuation link state observation if, for any initial condition (x_0, θ_0), and each link state $s_\ell \in \mathcal{S}$, there exists a link state-dependent gain $K_{(\infty,s_\ell)}$, such that $u_k^c = K_{(\infty,\theta_{k-1})} x_k$ is the stabilizing SF control input for (1).

Remark 11. The FSMC link model yields an MJLS model based on (16), and for MJLSs, the notions of MS stability, exponential MS stability, and stochastic stability are equivalent (Costa et al., 2005; Zacchia Lun, D'Innocenzo, & Di Benedetto, 2019). Thus, we recall only the definition of the MS stability.

Definition 12 (*Mean square stability*)**.** The system (1)–(3) is mean-square stable if there exist equilibrium points x_e and X_e, independent from the initial condition (x_0, θ_0), such that the following holds $\forall (x_0, \theta_0)$:

$$\lim_{k\to\infty} \|\mathbb{E}(x_k) - x_e\| = 0, \quad \lim_{k\to\infty} \|\mathbb{E}(x_k x_k^{\top}) - X_e\| = 0. \tag{28}$$

In (28), $\|\cdot\|$ indicates an arbitrary matrix norm.

5.1. MJLS model for stability analysis

The system (11)–(20) describes the behavior of the system (1)–(3) from the (remote) controller perspective. Stability analysis, however, requires a different perspective, considering each control message transmission outcome as the actuators see it. So, to apply Definition 12 to the system (11)–(16) from Proposition 4, couch the system in a Markovian framework by considering the augmented state $(x_{\tau_{(m+1)}}, \varphi_{\tau_{(m+1)}})$, with

$$\varphi_{\tau_{(m+1)}} \triangleq (\theta_{\tau_{(m+1)}}, \Delta_{\tau_{(m+1)}}, \theta_{\tau_{(m+1)}-\Delta_{\tau_{(m+1)}}-2}). \tag{29a}$$

Notice from (13) that

$$\theta_{\tau_{(m+1)}-\Delta_{\tau_{(m+1)}}-2} = \theta_{\tau_{(m)}-1}. \tag{29b}$$

The following augmented state is $(x_{\tau_{(m+2)}}, \varphi_{\tau_{(m+2)}})$, with

$$\varphi_{\tau_{(m+2)}} \triangleq (\theta_{\tau_{(m+2)}}, \Delta_{\tau_{(m+2)}}, \theta_{\tau_{(m+2)}-\Delta_{\tau_{(m+2)}}-2}), \tag{29c}$$

$$\theta_{\tau_{(m+2)}-\Delta_{\tau_{(m+2)}}-2} = \theta_{\tau_{(m+1)}-1}. \tag{29d}$$

Fig. 3 emphasizes the components of the augmented system's discrete states in black and the relevant transition probabilities for the time instances $\tau_{(m+1)}$ and $\tau_{(m+2)}$.

From the Markov property, chain rule of the probability, conditioned version of Bayes' theorem, and (29),

$$\mathbb{P}(\varphi_{\tau_{(m+2)}} = (s_{j_1}, n, s_{j_0}) \mid \varphi_{\tau_{(m+1)}} = (s_{i_1}, \ell, s_{i_0})) = \frac{e_{i_0}^{\top} P_1 P_0^{\ell} e_{j_0} e_{j_0}^{\top} P_1 e_{i_1}}{e_{i_0}^{\top} P_1 P_0^{\ell} P_1 e_{i_1}} e_{i_1}^{\top} P_0^{n} P_1 e_{j_1} \triangleq \mu_{((i_1,\ell,i_0),(j_1,n,j_0))}. \tag{30}$$

Notice from (20), (21), and (30) that for any (s_{i_1}, ℓ, s_{i_0}), $\sum_{j_1=1}^{N} \sum_{n\in\mathbb{Z}^{\geq}} \sum_{j_0=1}^{N} \mu_{((i_1,\ell,i_0),(j_1,n,j_0))} = 1$, i.e., the system (16) driven by (30) is an MJLS.

Lemma 13. *The system (1)–(3) under an arbitrary actuation link-state-dependent control* $u_k^c = K_{(\infty,\theta_{k-1})} x_k$ *is an MJLS described by (11)–(16), (29), and (30).*

Proof. It follows from Proposition 4, (29), (30), and noticing that both $x_{\tau_{(m+2)}}$ and $\varphi_{\tau_{(m+2)}}$ belong to the actuators' information set in $\tau_{(m+2)}$, which allows us to adopt a posteriori view of the MJLS and compute expectations backward in time.

The following section uses this MJLS to derive the easy-to-test condition of the closed-loop system stability for any given infinite-horizon control law.

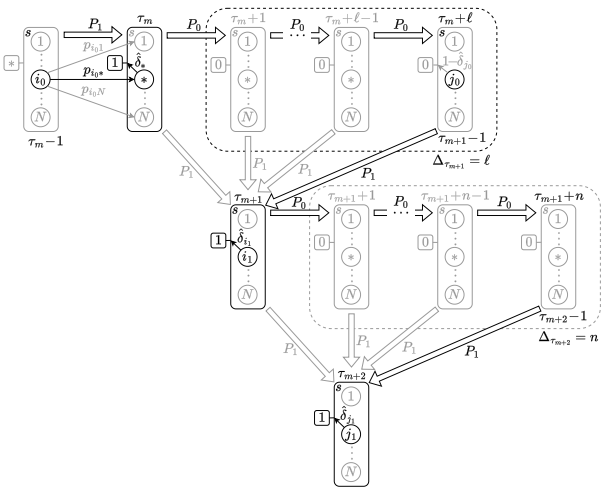

Fig. 3. The components of the augmented MJLS's discrete states for stability analysis. The solid rectangular boxes group the states of the FSMC (represented by circles) in specified time instances; the solid square boxes indicate the transmission outcomes, and the dashed rectangular boxes group the sequences of consecutive message dropouts. The thin arrows pinpoint the probabilities of specific events, while the thick arrows enclose the probabilities of all possible relevant events. The asterisks mark arbitrary values within their admissible sets.

5.2. Closed-loop system stability condition

We follow the standard MJLS approach tailored here for the problem at hand to derive the necessary and sufficient conditions for the closed-loop system stability. We highlight the technical details specific to the considered scenario and omit the presentation of the typical steps thoroughly explained in Costa et al. (2005, Ch. 3).

Consider an MJLS described by (11)–(16) and (30) for an arbitrary infinite-horizon SF control strategy with FSMC-dependent gain $K_{(\infty,\theta_{\tau_{(m)}-1})}$, where $m \in \mathbb{Z}^{\geq}$ and $\tau_{(m)}$ obeys (13). To obtain the recursive difference equation for the second moment of the system's state, let $1_{\{\varphi_{\tau_{(m+1)}}=(s_{i_1},\ell,s_{i_0})\}}$ be the indicator function specifying the membership (or non-membership) of a given element in the set. For notational convenience, let

$$M^{\tau_{(m+1)}}_{(i_1,\ell,i_0)} \triangleq \mathbb{E}\left(x_{\tau_{(m+1)}}x^{\top}_{\tau_{(m+1)}}1_{\{\varphi_{\tau_{(m+1)}}=(s_{i_1},\ell,s_{i_0})\}}\right). \tag{31}$$

$$\mathbb{E}\left(x_{\tau_{(m+1)}}x^{\top}_{\tau_{(m+1)}}\right) = \sum_{i_1=1}^{N}\sum_{\ell\in\mathbb{Z}^{\geq}}\sum_{i_0=1}^{N}\mathbb{E}\left(M^{\tau_{(m+1)}}_{(i_1,\ell,i_0)}\right).$$

To write expressions concisely, index the values of the ordered triples (v_1, v_2, v_3) representing the operational modes of the closed-loop system, with $1 \leq v_1, v_3 \leq N$ and $0 \leq v_2 \leq L$, using an invertible mapping $f : \mathbb{Z}^3 \to \mathbb{Z}$,

$$f(v_1, v_2, v_3) = N^2 v_2 + N(v_3 - 1) + v_1. \tag{32}$$

Then, the augmented system's discrete condition $\mathrm{c_i}$ will be a shorthand for (s_{i_1}, ℓ, s_{i_0}), with $f(i_1, \ell, i_0) = \mathrm{i}$.

Notice from (20) and (21) that for all $\mathrm{i}, \mathrm{j} \in \mathbb{Z}^{>}$, such that $f(i_1, \ell, i_0) = \mathrm{i}$, $f(j_1, n, j_0) = \mathrm{j}$, and $\mathrm{L} \triangleq (L+1)N^2$,

$$\sum_{\mathrm{j}=1}^{\mathrm{L}}\mu_{(\mathrm{i},\mathrm{j})} \geq 1 - \epsilon. \tag{33}$$

In the standard MJLS setting having system matrices depending on the present and not subsequent operational mode, the MS stability of the system without process noise is equivalent to the MS stability of the system with Gaussian process noise (Costa et al., 2005, Th. 3.33). The following sections also show this is the case for the considered setting described by (16) and (30).

Noiseless setting: Let $w_k = 0\ \forall k \in \mathbb{Z}^{\geq}$. (16), (29)–(32) $\Rightarrow$

$$M^{\tau(m+2)}_{(j_1,n,j_0)} = \mathbb{E}\left(x_{\tau(m+2)}x^{\top}_{\tau(m+2)}1_{\{\varphi_{\tau(m+2)}=(s_{j_1},n,s_{j_0})\}}\right) = \left(A^{n+1} + \Psi_{(n)}K_{(\infty,s_{j_0})}\right)\left(\sum_{\mathrm{i}=1}^{\mathrm{L}}M^{\tau(m+1)}_{\mathrm{i}}\mu_{(\mathrm{i},(j_1,n,j_0))}\right)\cdot \left(A^{n+1} + \Psi_{(n)}K_{(\infty,s_{j_0})}\right)^{\top} \tag{34}$$

$\forall\, \mathrm{i} \in \mathbb{Z}^{>}$ such that $f(i_1, \ell, i_0) = \mathrm{i}$ and $\mathrm{L} \triangleq (L+1)N^2$.

For notational convenience, let $\mathcal{M} \triangleq \left[\mu_{(\mathrm{i},\mathrm{j})}\right]^{\mathrm{L}}_{\mathrm{i},\mathrm{j}=1}$ and

$$\mathcal{L}_{\mathrm{j}} = \mathcal{L}_{(j_1,n,j_0)} \triangleq A^{n+1} + \Psi_{(n)}K_{(\infty,s_{j_0})}. \tag{35}$$

Denote by $\otimes$ the Kronecker product, by vec the matrix vectorization, and by vec^2 the matrix sequence vectorization formally defined as follows: $\forall M_{\mathrm{i}} \in \mathbb{R}^{n_x\times n_x}$,

$$\mathrm{vec}^2\left((M_{\mathrm{i}})^{\mathrm{L}}_{\mathrm{i}=1}\right) = \left[(\mathrm{vec}\,(M_1))^{\top}\cdots(\mathrm{vec}\,(M_{\mathrm{L}}))^{\top}\right]^{\top}. \tag{36}$$

Then, the vector form of (34) is

$$\mathrm{vec}^2\left(\left(M^{\tau(m+2)}_{\mathrm{j}}\right)^{\mathrm{L}}_{\mathrm{j}=1}\right) = \Lambda\mathrm{vec}^2\left(\left(M^{\tau(m+1)}_{\mathrm{i}}\right)^{\mathrm{L}}_{\mathrm{i}=1}\right), \tag{37}$$

where Λ is the MS stability verification matrix, and $I_{n_x^2}$ denotes the identity matrix of size n_x^2.

$$\Lambda = \left(\bigoplus_{\mathrm{j}=1}^{\mathrm{L}}\left(\mathcal{L}_{\mathrm{j}}\oplus\mathcal{L}_{\mathrm{j}}\right)\right)\left(\mathcal{M}^{\top}\oplus I_{n_x^2}\right) = \left[\left(\mathcal{L}_{\mathrm{j}}\oplus\mathcal{L}_{\mathrm{j}}\right)\mu_{(\mathrm{j},\mathrm{i})}\right]^{\mathrm{L}}_{\mathrm{i},\mathrm{j}=1} \tag{38}$$

The following theorem, where ρ indicates the spectral radius of a square matrix, i.e., the largest absolute value of its eigenvalues, provides the origin of the name for the matrix defined by (38).

Theorem 14. *The system (1)–(3) with $w_k = 0\ \forall k \in \mathbb{Z}^{\geq}$ and any given infinite-horizon control strategy satisfying (6) is mean-square stable if and only if $\rho(\Lambda) < 1$.*

Proof. From Lemma 13, proving the assertion for the system (11)–(16) coupled with (30) corresponds to proving it for the system (1)–(3) combined with (6). From (11)–(16), (29)–(36), the second moment of the MJLS evolves according to (37), where Λ, as defined by (38), is a fixed matrix. Hence, the standard MJLS approach holds and applying the steps from the proof of Costa et al. (2005, Th. 3.9) directly leads to the desired result. □

Contribution of the Gaussian process noise: Let

$$\mathcal{W}_{\mathrm{j}} = \mathcal{W}_{(j_1,n,j_0)} \triangleq \sum_{h=0}^{n}\left(A^{n-h}\right)\Sigma_W\left(A^{n-h}\right)^{\top}, \tag{39}$$

$$\psi_{\mathrm{i}}(\tau_{(m+1)}) \triangleq \mathbb{E}\left(1_{\{\varphi_{\tau_{(m+1)}}=\mathrm{c_i}\}}\right), \tag{40}$$

$$\mathcal{G}_{\mathrm{j}}(\tau_{(m+1)}) \triangleq \left(\sum_{\mathrm{i}=1}^{\mathrm{L}}\psi_{\mathrm{i}}(\tau_{(m+1)})\mu_{(\mathrm{i},\mathrm{j})}\right)\mathcal{W}_{\mathrm{j}}. \tag{41}$$

From (16), (29)–(32), (35), and Assumptions 1 and 3,

$$M^{\tau(m+2)}_{\mathrm{j}} = \mathcal{L}_{\mathrm{j}}\left(\sum_{\mathrm{i}=1}^{\mathrm{L}}M^{\tau(m+1)}_{\mathrm{i}}\mu_{(\mathrm{i},\mathrm{j})}\right)\mathcal{L}^{\top}_{\mathrm{j}} + \mathcal{G}_{\mathrm{j}}(\tau_{(m+1)}). \tag{42}$$

Moreover, Assumption 2 combined with (11)–(13) and (29) implies the ergodicity of the augmented Markov chain $\left\{\varphi_{\tau_{(m+1)}}\right\}_{m\in\mathbb{Z}^{\geq}}$, as formalized by the following.

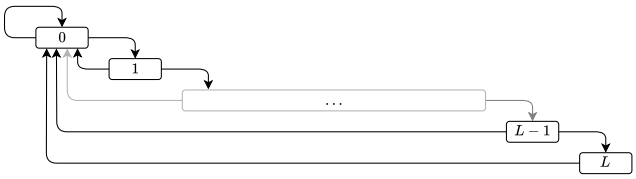

Fig. 4. Graphical representation of the stochastic process $\{\Delta_{\tau_{(m+1)}}\}$: the rectangles mark the process states labeled with the values each random variable $\Delta_{\tau_{(m+1)}}$ can assume, and the directed arcs between states indicate the non-zero probability transitions from the current to the next state.

Proposition 15. *If the Markov chain $\{\theta_k\}$ is ergodic, then the Markov chain $\left\{\varphi_{\tau_{(m+1)}}\right\}$ is also ergodic.*

Proof. To prove the assertion, show that the DTMC $\{\varphi_{\tau_{(m+1)}}\}$ has a finite number of states and consists entirely of one recurrent and aperiodic class[6] if the hypothesis on ergodicity of the Markov chain $\{\theta_k\}$ is satisfied. From (29), the state space of the DTMC $\{\varphi_{\tau_{(m+1)}}\}$ comprises the states of the finite-state Markov chain $\{\theta_k\}$ observed twice in different suitable time instants defined by (13) and the states of the stochastic process $\{\Delta_k\}$ described by (11) and observed in $\tau_{(m+1)}$. From (21) and (33), the probability of having $L+1$ consecutive control message dropouts is less than ϵ, the machine epsilon in the floating-point arithmetic. In other words, the probability of such an event is numerically zero, i.e., negligible in practice. Consequently, the stochastic process $\{\Delta_k\}$ has a finite number of states, $L+1$, and may consist entirely of one recurrent and aperiodic class. Fig. 4 shows the related graph and allows visually confirming that all the states communicate and are aperiodic if all the depicted arcs are present. The transition probabilities between the states of process $\{\Delta_k\}$ depend on the state of the FSMC that evolves according to the Markov chain $\{\theta_k\}$. Observing that an FSMC cannot have $\hat{\delta}_i$ equal to zero (or one) in all its states $\{s_i\}_{i=1}^N$, conclude that the ergodic property of $\{\theta_k\}$ ensures that all the directed arcs in Fig. 4 are indeed present, i.e., all the depicted transitions are always possible. A direct consequence is that the finite-state DTMC $\{\varphi_{\tau_{(m+1)}}\}$ consists entirely of one class of states that is both recurrent and aperiodic, implying its ergodicity. □

A direct consequence is the following.

Theorem 16. *Under Assumption 2, the system (1)–(3) with any given infinite-horizon control strategy satisfying (6) is mean-square stable if and only if $\rho(\Lambda) < 1$.*

Proof. By Lemma 13, the system (11)–(16) and (30) is trace-equivalent to the system (1)–(3) governed by (6). So, we focus only on the MJLS described by (11)–(16) and (30). Proposition 15 implies the existence of the steady-state probability distribution $\psi_{\mathrm{i}} \triangleq \lim_{m\to\infty} \psi_{\mathrm{i}}(\tau_{(m+1)})$ independent of the initial distribution $\psi_{\mathrm{i}}(\tau_{(1)})$ so that $\mathcal{G}_{\mathrm{j}} \triangleq \left(\sum_{\mathrm{i}=1}^{\mathrm{L}} \psi_{\mathrm{i}}\, \mu_{(\mathrm{i},\mathrm{j})}\right) \mathcal{W}_{\mathrm{j}}$. Recalling (34)–(42) and repeating the steps of the proofs in Costa et al. (2005, Sec. 3.4.2) leads to $x_e = 0$, $X_e = \mathrm{vec}^{-2}\left(\left(I_{\mathrm{Ln}_x^2} - \Lambda\right)^{-1} \mathrm{vec}^2\left(\left(\mathcal{G}_{\mathrm{j}}\right)_{\mathrm{j}=1}^{\mathrm{L}}\right)\right)$ when $\rho(\Lambda) < 1$, and the desired result follows. □

Section 7 extensively validates Theorem 16 on a numerical case study, while the following section focuses on designing an optimal infinite-horizon SF control strategy for a generalized dropout compensation.

[6] See, e.g., Gallager (2013) for the definitions and insights.

6. Optimal infinite-horizon LQR

If the system (1) is stabilizable according to Definition 10, the coupled difference Riccati equations (CDREs) (24) converge, resulting in the coupled algebraic Riccati equations (CAREs), with the indices k and $k+1+h$ substituted by ∞, and $\xi_\infty = 0$ since there is no end of the time horizon. Similarly to the standard MJLS case, at most, one stabilizing solution of CAREs exists, which coincides with the maximal solution of an equivalent convex programming problem. The proof of the uniqueness and asymptotic convergence is on the lines of Costa et al. (2005, Appendix A—Thms A.10 and A.12, Lemma A.14, and Prop. A.23) and does not present technical challenges specific to the wireless networked control scenario. Thus, this section omits the detailed proof of the uniqueness and asymptotic convergence and directly presents the solution to the CAREs in terms of LMIs:

$$\breve{\mathcal{X}}_{(s_i)} = \underset{\mathcal{X}_{(\infty,s_i)}}{\arg\max}\, \mathrm{tr}\left(\sum_{i=1}^{N} \mathcal{X}_{(\infty,s_i)}\right) \tag{43a}$$

subject to

$$\begin{bmatrix} -\mathcal{X}_{(\infty,s_i)} + \mathcal{A}_{(\infty,s_i)} & \mathcal{C}_{(\infty,s_i)}^\top \\ \mathcal{C}_{(\infty,s_i)} & \mathcal{B}_{(\infty,s_i)} \end{bmatrix} \succeq 0, \tag{43b}$$

$$\mathcal{X}_{(\infty,s_i)} \succeq 0, \quad \mathcal{B}_{(\infty,s_i)} \succ 0, \tag{43c}$$

with the terms in (43) defined by (24) for $k=\infty$, and $\xi_\infty = 0$ for all $s_i \in \mathcal{S}$.

For notational conciseness, refer to (24a) and (24b) as $\breve{\mathcal{C}}_{(s_i)}$ and $\breve{\mathcal{B}}_{(s_i)}$ when their expressions involve the solution, $\left\{\breve{\mathcal{X}}_{(s_i)}\right\}$, of the LMIs (43).

To provide a closed-form expression of the long-run average cost, define the initial probability distribution of the packet error bursts that end in a specific FSMC's state:

$$\pi_{(h,j)}(0) \triangleq \sum_{i=1}^{N} \vartheta_i e_i^\top \varsigma_{(h,j)} \tag{44a}$$

results in $\{\pi_{(h,j)}(0)\}$. It evolves as follows.

$$\pi_{(\ell,i)}(k+1) \triangleq \sum_{h=0}^{L}\sum_{j=1}^{N} \pi_{(h,j)}(k) e_j^\top \varsigma_{(\ell,i)}. \tag{44b}$$

Notice (from the proof of Proposition 15) that Assumption 2 implies the existence of the steady-state distribution:

$$\pi_{(\ell,i)} \triangleq \lim_{k\to\infty} \pi_{(\ell,i)}(k). \tag{44c}$$

Theorem 17. *Given the solution $\left\{\breve{\mathcal{X}}_{(s_i)}\right\}$ of the LMIs (43) under Assumption 2, the resulting infinite-horizon LQR law defining (10) for a stabilizable system (1) is*

$$\breve{u}_k^c = K_{(\infty,\theta_{k-1})} x_k, \tag{45a}$$

$$K_{(\infty,s_i)} = -\breve{\mathcal{B}}_{(s_i)}^{-1} \breve{\mathcal{C}}_{(s_i)} \tag{45b}$$

for $\theta_{k-1} = s_i$, and the optimal cost that minimizes (9)

$$J_\infty^\star = \sum_{h=0}^{L}\sum_{j=1}^{N} \pi_{(h,j)} \left(\sum_{r=1}^{h}\sum_{\nu=0}^{r-1} \mathrm{tr}(A^{\nu\top} Q A^\nu \Sigma_W) + \sum_{\nu=0}^{h} \mathrm{tr}(A^{\nu\top} \breve{\mathcal{X}}_{(s_j)} A^\nu \Sigma_W)\right). \tag{45c}$$

Proof. This proof is similar to the proof of Costa et al. (2005, Th. 4.6). The LQR law in (45a) complies with (6) so that $\breve{u}_k^c \in \mathcal{U}_\infty$. From the general MJLSs theory outlined at the beginning of Section 6, the stabilizability of the system (1) ensures that the CDREs

(24) converge into the CAREs. If the LMIs' (43) solution exists, it provides the maximal solution to the CAREs, which coincides with the unique stabilizing solution. Then, (45b) follows. From (9), (19), (20), (25), (27), (44), and $\{\mathcal{X}_{(k,s_i)}\} = \{\breve{\mathcal{X}}_{(s_i)}\}$ for all k,

$$J^{\star}_{\infty} = \limsup_{T\to\infty} \frac{1}{T} \sum_{k=0}^{T-1} \sum_{h=0}^{L} \sum_{j=1}^{N} \pi_{(h,j)}(k) \Bigg(\sum_{r=1}^{h} \sum_{\nu=0}^{r-1} \mathrm{tr}(A^{\nu\top} Q A^{\nu} \Sigma_W) + \sum_{\nu=0}^{h} \mathrm{tr}(A^{\nu\top} \breve{\mathcal{X}}_{(s_j)} A^{\nu} \Sigma_W) \Bigg),$$

which results in (45c) and concludes the proof. □

Remark 18. Both finite- and infinite-horizon gains (23) and (45b) depend on the dropout compensation factor Φ. Section 7.6 examines the impact of the dropout compensation factor on the closed-loop stability and control cost in a numerical case study. An analytical derivation of the optimal Φ minimizing the control cost with or without stability constraints is an important future research direction enabled by the results of this paper. To this end, the approach of Yu and Fu (2015) to the optimal dropout compensator design is a good starting point, from which the tedious matrix derivation over structured matrices of numerous terms involving matrix products of structured and unstructured matrices, some of which are elevated to arbitrarily high powers, must be addressed in the FSMC-state-dependent control setting.

7. Numerical case study

This section numerically validates the theoretical results of Theorems 9, 16, and 17 on the case study of the rotary inverted pendulum (controlled remotely through a wireless link) chosen to thoroughly examine the impact of a scalar general dropout compensation factor $\phi_1 \in [0, 1]$. Notice that $n_u = 1$ implies that $\Phi = \phi_1$, i.e., a scalar. This choice allows us to plot the spectral radius of the MS stability verification matrix and long-run average cost as a function of ϕ_1 in Figs. 12 and 13.

7.1. System model and parameters

The pendulum model and parameters are from Apkarian, Karam, and Lévis (2020). The system state consists of the rotary arm and pendulum angles and their derivatives, i.e., the corresponding angular velocities. The linearization around the unstable equilibrium point and the zero-order hold discretization with a sampling rate of 12 Hz produces the following discrete-time system matrices.

$$A = \begin{bmatrix} 1 & 0.224 & 0.055 & 0.004 \\ 0 & 1.369 & -0.028 & 0.090 \\ 0 & 4.994 & 0.391 & 0.167 \\ 0 & 8.618 & -0.634 & 1.270 \end{bmatrix}, \quad B = \begin{bmatrix} 0.227 \\ 0.218 \\ 4.944 \\ 4.820 \end{bmatrix}.$$

This linear model is suitable for the ISA100.11a communication protocol (IEC 62734, 2014, Clause 9.1.9.1.3) and holds for the small angles from the vertical, e.g., less than 0.175 rad.

Consider the system affected by a Gaussian white process noise with a covariance matrix $\Sigma_w = 2.5 \cdot 10^{-9} I_4$. The state-weighting and input-weighting matrices defining the LQR costs are $Q = \bigoplus\{1, 5, 1, 1\}$ and $R = 10$. The controller aims to balance the pendulum in the upright position corresponding to the inverted pendulum angle equal to zero at the lowest cost.

The controller sends the messages to actuators via a wireless link modeled as the following FSMC.

$$P_c = \begin{bmatrix} 0.257 & 0.027 & 0.032 & 0.684 \\ 0.182 & 0.023 & 0.028 & 0.767 \\ 0.172 & 0.022 & 0.027 & 0.779 \\ 0.058 & 0.010 & 0.012 & 0.920 \end{bmatrix}, \quad \hat{\delta} = \begin{bmatrix} 0.026 \\ 0.375 \\ 0.634 \\ 0.995 \end{bmatrix}^{\top}. \tag{46}$$

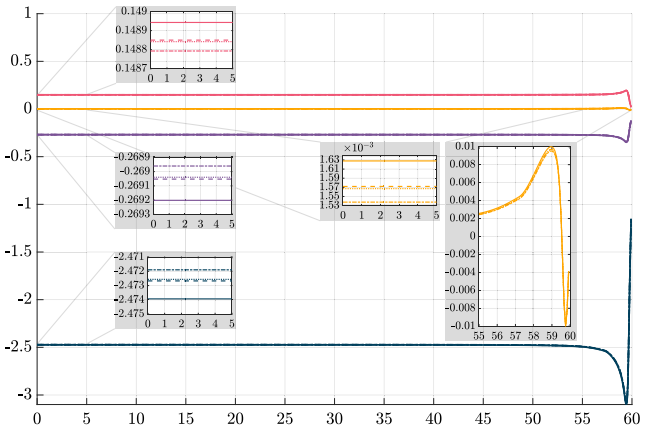

Fig. 5. Values of the finite-horizon SF gain components in time: solid lines indicate the gain components for the fourth FSMC state, s_4, dashed lines refer to the third state, s_3, dotted lines identify the components of gain for the second channel state, s_2, and dash-dotted lines represent the gain components for the first FSMC state, s_1. Orange color identifies the gain component acting on the rotary arm angle, blue singles out the component affecting the pendulum angle, violet indicates the component adjusting the rotary arm angular velocity, and red pinpoints the component varying the pendulum angular velocity. Viewing the plot backwards shows a transitory of around five seconds followed by a steady convergence in the remaining time.

This FSMC accurately describes the successful control message deliveries over IEEE 802.15.4-based links under Wi-Fi interference (Zacchia Lun et al., 2024) and derives from a wireless networked control system co-design framework in Zacchia Lun et al. (2020).

7.2. Finite-horizon LQR example

To showcase the finite-horizon control strategy in Theorem 9, consider the time horizon $T = 60$ seconds (corresponding to 720 samples) and the dropout compensation factor $\phi_1 = 0.921$. See Section 7.6 for a motivation for using this value of ϕ_1 as the one producing the most stable behavior in infinite-horizon control setting. From (23), the initial SF control gains are the following.

$$K_{(0,1)} = [\,0.001538 \quad -2.471896 \quad 0.148793 \quad -0.268961\,],$$
$$K_{(0,2)} = [\,0.001567 \quad -2.472563 \quad 0.148842 \quad -0.269040\,],$$
$$K_{(0,3)} = [\,0.001572 \quad -2.472673 \quad 0.148850 \quad -0.269053\,],$$
$$K_{(0,4)} = [\,0.001628 \quad -2.473934 \quad 0.148943 \quad -0.269201\,].$$

Fig. 5 depicts the gain components' evolution throughout the time horizon and highlights their convergence to the initial ones, as shown by constant values on the zoomed-in plots for the first 5 s (i.e., final seconds backwards in time). It indicates a possible convergence of CDREs to CAREs and the system's stabilizability, as detailed in Section 6 and confirmed in Section 7.3.

Assuming the uniform initial probability distribution of the FSMC's states (i.e., $\vartheta_i = 0.25$ for all s_i) and the initial pendulum angle and angular velocity of around 10° and 44°/s so that $x_0 = [0\ 0.174\ 0\ 0.767]^{\top}$, the cost of the control given by (25) is $J^{\star}_T(x_0) = 1988.980076$. The initial system state in the unstable equilibrium point $x^{\star}_0 = [0\ 0\ 0\ 0]^{\top}$ would produce $J^{\star}_T(x^{\star}_0) = 3.416528$, corresponding to the contribution of the second addend in (25) to $J^{\star}_T(x_0)$.

7.3. Infinite-horizon LQR example

Notice that the TPM P_c in Section 7.1 is fully connected, implying that Assumption 2 is satisfied. Consider the dropout compensation factor $\phi_1 = 0.921$ again. Solving the LMIs (43) in the

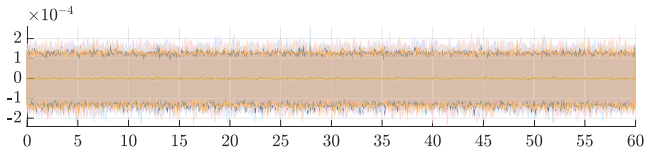

Fig. 6. Process noise component statistics over 60 seconds from 500 independent traces: orange color indicates the component perturbing the rotary arm angle, blue identifies the process noise component affecting the pendulum angle, violet singles out the component disturbing the rotary arm angular velocity, and red pinpoints the component varying the pendulum angular velocity. All median values are close to zero, 95% of observed values are between ± 0.0001, and all the values are greater than -0.0003 and less than 0.0003.

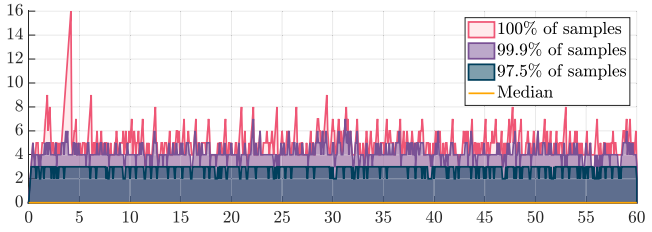

Fig. 7. Control-packet error burst length statistics over 60 seconds from a batch of 2000 traces: the median values (in orange) are all zero, 97.5% of observed values (in blue) are always less than or equal to two, 99.9% (in violet) is less than or equal to 7, and the maximal values (in red) are predominantly below 8, but equal 9 three times, and 16 once.

Robust Control Toolbox for MATLAB (Balas, Chiang, Packard, & Safonov, 2023) via its solver `mincx` and applying Theorem 17 produces the infinite-horizon gains $\{K_{(\infty,s_i)}\}$ equal to the initial SF gains $\{K_{(0,s_i)}\}$ in Section 7.2 and the optimal long-run average cost $J^{\star}_{\infty} = 0.007692$. The spectral radius of the MS stability verification matrix (38) with these infinite-horizon gains is $\rho(\Lambda) = 0.979943$. By Theorem 16, the closed-loop system is mean-square stable.

7.4. Monte Carlo simulation setup

To empirically assess the proposed control strategy, we generated 500 independent process noise trace samples described in Fig. 6 and 2000 independent control-packet error burst length evolution traces summarized in Fig. 7. Each packet error burst trace was the output of the FSMC (46). Thus, we obtained one million independent samples of the stochastic processes involved by considering every combination of the process noise trace and FSMC evolution. Notably, the packet error burst traces in Fig. 7 are from one of 1000 batches of 2000 traces each, which we selected because of the longest observed burst at the very beginning of the considered time interval of 60 seconds, a valuable feature for illustrating the system resilience to particularly long consecutive packet error intervals. Furthermore, the selected batch was the only one having 16 consecutive control packet errors, which was the most extended observed packet error burst.[7]

7.5. Plant dynamics statistics

To highlight the impact of the control packet dropouts and process noise, we computed the plant's closed-loop dynamics under the proposed infinite-horizon control strategy from Section 7.3 starting from the unstable equilibrium point $x^{\star}_0 = [0\ 0\ 0\ 0]^{\top}$ as the system's initial state for each stochastic sample from Section 7.4.

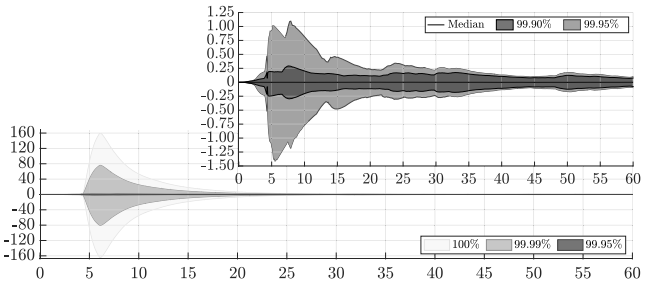

Fig. 8. Statistics of the rotary arm angle dynamics.

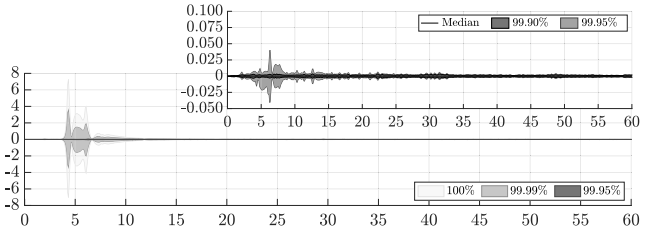

Fig. 9. Statistics of the pendulum angle dynamics.

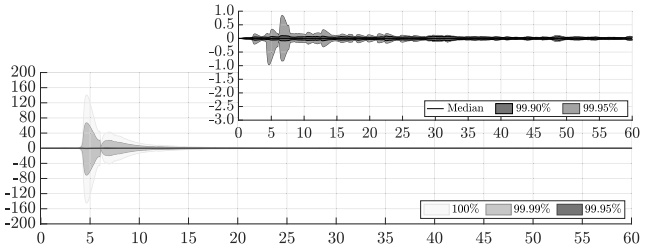

Fig. 10. Statistics of the rotary arm angular velocity.

Figs. 8–11 show the observed system's behavior statistics. The lower part of each figure underlines the effect of the most prolonged packet error burst of length 16 combined with different realizations of process noise, accounting for 500 (0.05% of total) samples. It shows that even under the most unfavorable combination of the control packet dropout and process noise, the closed-loop system dynamics always return to the unstable equilibrium point, as expected from a mean-square stable system. The lower part of Fig. 9 also indicates that in practical applications, particularly long control packet error bursts may bring the system state outside the valid linearization region (± 0.175 radians for the rotary inverted pendulum in the exam), an issue outside the MS stability. The upper part of each figure zooms in on the remaining 99.95% of samples, showing that even the improbably long control packet error burst combined with a slight process noise does not create any stability issues, and shorter packet error bursts (combined with any realization of the process noise) do not create any issue either. In particular, under the proposed control strategy, 99.95% of examined pendulum angle traces remain within 0.05 radians from the vertical, as shown in the upper part of Fig. 9.

To assess the long-run average cost, we first exclude as outliers the execution traces obtained with the control packet error burst of length 16 since the estimated probability of the related event is below 0.0000005, much lower than the probability of any other considered event. Then, as expected, the 60-second-run average cost over 99.95% of samples is 0.000163134, significantly lower

[7] The most common longest packet error burst in a batch was of length 9 (38.6% of batches), closely followed by the one of length 10 (35.5%); the others were of length 8 (7.2%), 11 (12.8%), 12 (3.9%), 13 (1.3%), and 14 (0.6%).

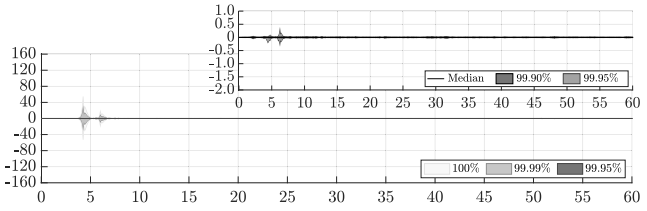

Fig. 11. Statistics of the pendulum angular velocity dynamics.

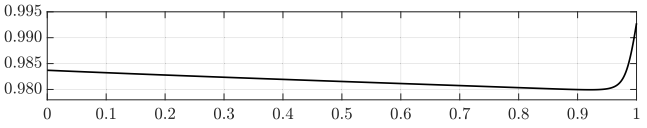

Fig. 12. The spectral radius of the MS stability verification matrix, $\rho(\Lambda)$, as a function of the dropout compensation factor ϕ_1 for the rotary inverted pendulum under the proposed infinite-horizon LQR.

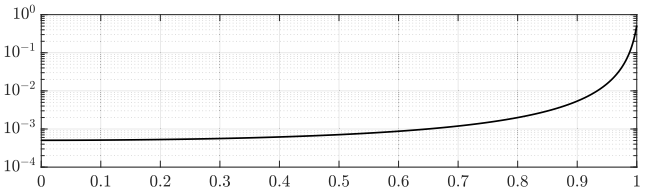

Fig. 13. Long-run average cost $J^{\star}_{\infty}(\phi_1)$ for the rotary inverted pendulum under the proposed infinite-horizon LQR.

than $J^{\star}_{\infty}$ in Section 7.3 since it neglects the costly contribution of control packet error bursts of length greater than 9. Considering also the 250 less expensive traces with the packet error burst of length 16 brings the average cost over 99.975% of samples to 0.007333882, slightly lower than $J^{\star}_{\infty} = 0.007691683$. Finally, the 60-second-run average cost over all samples in the presented butch is 0.110421117, much higher than the long-run average.

This data confirms that the presented butch represents well the system behavior statistics, identifying both very extreme and typical execution traces. It also corroborates the MS stability of the closed-loop system, thus validating the result of Theorem 16.

7.6. Impact of the dropout compensation factor

An essential application of the presented theoretical results is assessing the closed-loop system stability and control cost for different control strategies and dropout compensation gains. Fig. 12 shows the values of $\rho(\Lambda)$ defined by (38) for varying values of $\Phi = \phi_1$. Notice that $\rho(\Lambda)$ values decrease from 0.983706 in 0 to 0.979943 in 0.921 and then monotonically increase to 0.992784 in 1. This analysis indicates that $\phi_1 = 0.921$ provides the most stable closed-loop behavior in the mean-square sense, ensuring the system's robustness to prolonged control packet error bursts. Fig. 13 presents the long-run average cost of the proposed infinite-horizon LQR for varying values of $\Phi = \phi_1$. This cost increases monotonically in ϕ_1, passing from 0.000505 in 0 to 0.000511 in 0.1, 0.000562 in 0.3, 0.000710 in 0.5, 0.001195 in 0.7, 0.005389 in 0.9, and 0.519529 in 1. The long-run average cost and MS stability analyses reveal that the dropout compensation factors between 0 and 0.921 provide the trade-off between the two metrics, with particular choices depending on the design's priorities.

The zero-input dropout compensation strategy ($\phi_1 = 0$) provides the lowest long-run average cost for the rotary inverted pendulum. The following section shows that with this dropout

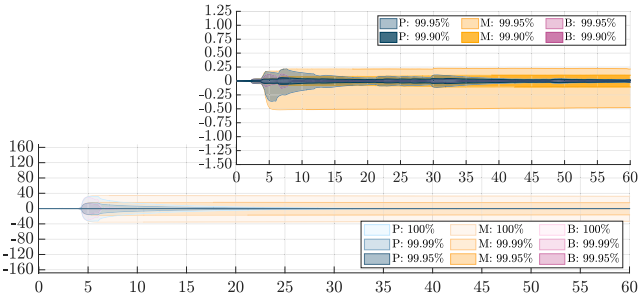

Fig. 14. Statistics of the rotary arm angle dynamics.

compensation, the proposed LQR outperforms the existing wireless control strategies in the MS stability terms (at the price of higher complexity of the CAREs).

7.7. Comparative analysis

For the feedback control over lossy communication links with zero-input dropout compensation, Schenato et al. (2007) and Impicciatore et al. (2024) presented alternative LQR strategies assuming the packet dropout dynamics are realizations of the Bernoulli or FSMC processes.

The channel-state-independent LQR gain from Schenato et al. (2007) relies on the solution of the modified Riccati equation for a specific value of the control packet arrival probability. The successful packet arrival probability for the FSMC (46) is 0.908862, producing the following LQR gain for the rotary inverted pendulum from Section 7.1.

$$K^{B} = [\,0.048425 \quad -4.419243 \quad 0.283052 \quad -0.495964\,].$$

By (38), applying K^{B} produces $\rho\left(\Lambda^{B}\right) = 1.042846$, i.e., unstable system behavior.

The wireless channel-state-dependent LQR gains from Impicciatore et al. (2024) come from the solution of the CAREs that account only for the expected immediate outcome of the control message transmission without taking explicit care of possible packet error bursts. The resulting gains are

$$K^{M}_{(1)} = [\,-0.000285 \quad -4.581419 \quad 0.271732 \quad -0.493482\,],$$
$$K^{M}_{(2)} = [\,-0.000649 \quad -4.446127 \quad 0.266240 \quad -0.483612\,],$$
$$K^{M}_{(3)} = [\,-0.000597 \quad -4.425511 \quad 0.265311 \quad -0.482016\,],$$
$$K^{M}_{(4)} = [\,0.000162 \quad -4.229347 \quad 0.255946 \quad -0.466310\,].$$

From (38), these gains maintain an MS stability with $\rho\left(\Lambda^{M}\right) = 0.999749$.

Finally, the proposed LQR gains from Theorem 17 are

$$K^{P}_{(1)} = [\,0.011000 \quad -4.528464 \quad 0.275168 \quad -0.494649\,],$$
$$K^{P}_{(2)} = [\,0.011208 \quad -4.528800 \quad 0.275254 \quad -0.494734\,],$$
$$K^{P}_{(3)} = [\,0.011242 \quad -4.528856 \quad 0.275268 \quad -0.494748\,],$$
$$K^{P}_{(4)} = [\,0.011634 \quad -4.529491 \quad 0.275429 \quad -0.494908\,]$$

for $\phi_1 = 0$. Their $\rho\left(\Lambda^{P}\right) = 0.983706$, indicating better mean-square stable performance, with faster return to unstable equilibrium point after perturbations from control packet error bursts and process noise. Moreover, the long-run average cost is 0.000505.

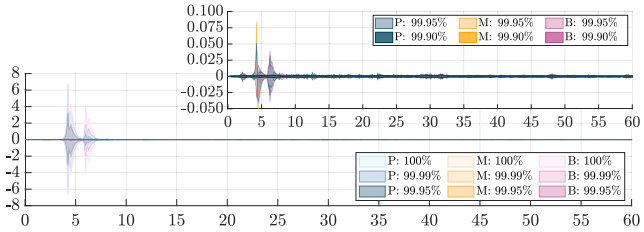

Fig. 15. Statistics of the pendulum angle dynamics.

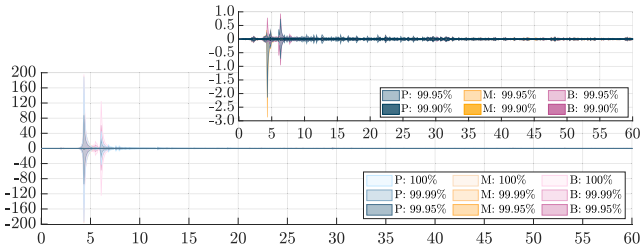

Fig. 16. Statistics of the rotary arm angular velocity.

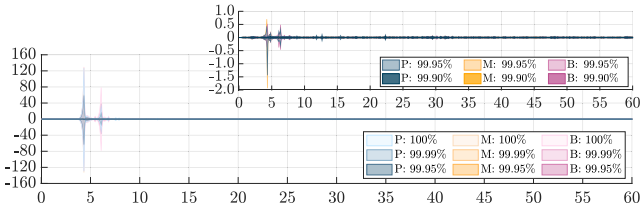

Fig. 17. Statistics of the pendulum angular velocity dynamics.

We numerically validate this analysis via Monte Carlo simulations in Section 7.4.

Figs. 14–17 show the system's behavior statistics for the three LQR strategies, where P indicates the proposed controller (in shades of blue), M identifies the Markovian controller from Impicciatore et al. (2024) (in shades of orange), and B marks the Bernoullian controller from Schenato et al. (2007) (in shades of mulberry). Fig. 14 highlights much faster convergence of the rotary arm angle to the origin for the proposed controller compared to the Markovian. The Bernoullian control strategy exhibits the fastest convergence of the rotary arm angle, which translates into the highest angular velocities and additional oscillations displayed in Fig. 16. Moreover, Figs. 15 and 17 illustrate that the Bernoullian controller strays the pendulum the most from the unstable equilibrium point and introduces deeper oscillations of the pendulum's angle and velocity, indicating less stable behavior. The proposed controller, instead, maintains the pendulum angle and velocity closer to the origin and efficiently dampens the oscillations.

Similarly to Section 7.5, we computed the 60-second-run average cost of the LQR strategies over different percentages of closed-loop system evolution traces, summarized in Table 1. The Bernoullian strategy achieves the lowest average cost over 99.95% of samples that exclude the packet error burst of length 16. The proposed LQR strategy maintains the best mean-square stable behavior at a lower cost than the average cost of the Markovian strategy. Furthermore, the proposed approach provides the lowest cost over 99.975% and 100% of samples, i.e., those considering packet error bursts longer than 9.

Finally, as expected from the analysis in Section 7.6, the proposed LQR strategy with the zero-input dropout compensation strategy has a smaller long-run average and observed 60-second-run average costs compared to the proposed strategy with the dropout compensation factor of 0.921 but presents less stable mean-square behavior, confirmed by the execution traces in Figs. 8–11 and 14–17 and a higher value of the MS stability verification matrix spectral radius, $\rho(\Lambda)$.

Table 1
Sixty-second-run average costs of different LQR strategies.

Controller	99.95%	99.975%	100%
Bernoullian	0.000012134	0.001012662	0.014424479
Markovian	0.000057042	0.005220157	0.078928154
Proposed	0.000015449	0.000892386	0.013577407

8. Conclusions

This paper introduced a functional Markov jump linear system modeling of wireless networked control systems with a generalized control message dropout compensation over lossy actuation links modeled by finite-state Markov channels. We envisage extending it to the robust control setting by considering the polytopic time-inhomogeneous Markov channels and different control strategies.

Acknowledgments

This work was supported in part by the Italian government through the Interministerial Committee for Economic Planning (CIPE), Italy under Resolution 70/2017 (Centre EX-Emerge) and in part by the EU through the DigInTraCE project under grant 101091801, the Resilient Trust project under grant 101112282, and the Italian National Recovery and Resilience Plan of NextGenerationEU, Italy under project MoVeOver/SCHEDULE with CUP J33C22002880001.

Appendix. Proof of Theorem 9

Due to the length constraint of the paper, this section only outlines the main steps of the proof that underwent peer review and is available in Zacchia Lun, Smarra, and D'Innocenzo (2025). The proof follows the *dynamic programming* approach in Bellman's optimization formulation: we define the cost-to-go $\forall k \in \mathbb{Z}^{\geq}$ as

$$J_T^\star(x_k, \theta_{k-1}) \triangleq \min_{(u_t^c \in \mathcal{U}_T)_{t=k}^{T-1}} \mathbb{E}\left(\sum_{t=k}^{T-1}\left(x_t^\top Q x_t + u_t^\top R u_t\right) + x_T^\top Q x_T \mid \mathcal{I}_k\right)$$

so that $k = 0$ provides the optimal cost.

From the tower property of the conditional expectation, (5), (7), and (26), $J_T^\star(x_0) = \sum_{i=1}^N \vartheta_i J_T^\star(x_0, s_i)$. Therefore, showing that

$$J_T^\star(x_k, \theta_{k-1}) = x_k^\top \mathcal{X}_{(k,\theta_{k-1})} x_k + g_{(k,\theta_{k-1})}, \tag{A.1}$$

with $\mathcal{X}_{(k,\theta_{k-1})} \succeq 0$ (positive semi-definite) and $g_{(k,\theta_{k-1})} \geq 0$, is the core of this proof. The main technical challenge lies in transition probabilities (20b) defined for the time instances $\tau_{(m)}$ and $\tau_{(m+1)}$ in $\mathcal{T}$, which are unknown to the controller beforehand. We proceed by *backward induction*. From (5), the optimal control policy $\check{\mathbf{u}}_T^c$ (8) produces the *terminal cost* $J_T^\star(x_T, \theta_{T-1}) = \mathbb{E}\left(x_T^\top Q x_T \mid \mathcal{I}_T\right) = x_T^\top Q x_T$. Thus, (A.1) holds in the base case. Furthermore, with $\theta_{T-1} = s_i$, the terminal cost expression implies (24d) and $g_{(T,s_i)} = 0$ for any $s_i \in \mathcal{S}$. For the *induction step*, we assume (A.1) holds for $k+1 = \min\{\tau_{(m+1)}, T\}$, with $\tau_{(m+1)}$ being the time of the first successful control message transmission following an arbitrary k that may exceed the time horizon T. Let $\tau_{(m)}$ indicate the time of the last successful control message transmission preceding $k+1$. From (13), $k = \min\{\tau_{(m)} + \Delta_{\tau_{(m+1)}}, T-1\}$. From the tower property of the conditional expectation and cost-to-go definition,

$J_T^\star(x_{\tau_{(m)}}, \theta_{\tau_{(m)}-1}) = \min_{\{u_t^c \in \mathcal{U}_T\}_{t=\tau_{(m)}}^k} \mathbb{E}\Big(\sum_{t=\tau_{(m)}}^k \left(x_t^\top Q x_t + u_t^\top R u_t\right) + J_T^\star(x_{k+1}, \theta_k) \mid \mathcal{I}_{\tau_{(m)}}\Big)$. From the inductive hypothesis, the linearity of the expectation, (1), (5), (6), (13)–(16), Assumptions 1 and 3, the cyclic property of the trace, and the fact that w_k is a white Gaussian process with zero mean and covariance matrix Σ_w, the cost-to-go is the minimum in $K_{(\tau_{(m)},s_i)}$, with summations of up to $k - \tau_{(m)}$ terms, as shown by Zacchia Lun et al. (2025, Eq. (A.8)). $\tau_{(m)} \leq T - 1$. From (21), $k - \tau_{(m)}$ is a bounded discrete stochastic variable. $\xi_{\tau_{(m)}} \triangleq \max\{0, \tau_{(m)} + 1 + L - T\} \Rightarrow \max(k - \tau_{(m)}) = L - \xi_{\tau_{(m)}}$. From (17)–(20), the terms independent of $K_{(\tau_{(m)},s_i)}$ and $x_{\tau_{(m)}}$ become $g_{(\tau_{(m)},s_i)}$ as in (27), while the terms independent of $K_{(\tau_{(m)},s_i)}$ form $\mathcal{A}_{(\tau_{(m)},s_i)}$ as in (24e). Defining the terms $\mathcal{B}_{(\tau_{(m)},s_i)}$ and $\mathcal{C}_{(\tau_{(m)},s_i)}$ as in (24a) and (24b) and performing the matrix differentiation to find stationary points in $K_{(\tau_{(m)},s_i)}$ yields (23), (24c), and (A.1) with $\tau_{(m)}$ in place of k, which implies (25) for $\tau_{(m)} = 0$. Rewriting (24c) in a form similar to Zacchia Lun et al. (2025, Eq. (A.10)) proves that $\mathcal{X}_{(\tau_{(m)},s_i)} \succeq 0$. As a covariance matrix, $\Sigma_w \succeq 0$, so $g_{(\tau_{(m)},s_i)} \geq 0$. Since at each transmission time, the controller selects the SF gain (23) under the assumption that it will be successfully received, and $\tau_{(m)}$ formalizes this assumption via (13a), this proof provides the expressions in $\tau_{(m)}$. Writing the expressions in k instead of $\tau_{(m)}$ results in (22)–(27) and concludes the proof. □

References

Apkarian, J., Karam, P., & Lévis, M. (2020). *Inverted Pendulum Experiment for MATLAB/Simulink Users: Student workbook*, Quanser, Inc.

Balas, G., Chiang, R., Packard, A., & Safonov, M. (2023). Robust Control Toolbox User's Guide, Ver. 23.2 (R2023b). *MathWorks Matlab*.

Battilotti, S., Cacace, F., d'Angelo, M., Germani, A., & Sinopoli, B. (2019). LQ non-Gaussian regulator with Markovian control. *IEEE Control Systems Letters*, *3*(3), 679–684. http://dx.doi.org/10.1109/LCSYS.2019.2916287.

Cetinkaya, A., Ishii, H., & Hayakawa, T. (2017). Networked control under random and malicious packet losses. *IEEE Transactions on Automatic Control*, *62*(5), 2434–2449. http://dx.doi.org/10.1109/TAC.2016.2612818.

Costa, O. L. V., Fragoso, M. D., & Marques, R. P. (2005). *Discrete-time Markov jump linear systems*. Springer London, http://dx.doi.org/10.1007/b138575.

Ding, B. (2011). Stabilization of linear systems over networks with bounded packet loss and its use in model predictive control. *Automatica*, *47*(11), 2526–2533. http://dx.doi.org/10.1016/j.automatica.2011.08.038.

Eisen, M., Rashid, M. M., Gatsis, K., Cavalcanti, D., Himayat, N., & Ribeiro, A. (2019). Control aware radio resource allocation in low latency wireless control systems. *IEEE Internet Things Journal*, *6*(5), 7878–7890. http://dx.doi.org/10.1109/JIOT.2019.2909198.

Gallager, R. G. (2013). *Stochastic processes: theory for applications*. Cambridge University Press, http://dx.doi.org/10.1017/CBO9781139626514.

Goldsmith, A. (2005). *Wireless Communications*. Cambridge University Press, http://dx.doi.org/10.1017/CBO9780511841224.

Gonçalves, A. P. C., Fioravanti, A. R., & Geromel, J. C. (2010). Markov jump linear systems and filtering through network transmitted measurements. *Signal Processing*, *90*(10), 2842–2850. http://dx.doi.org/10.1016/j.sigpro.2010.04.007.

Gupta, V., Dana, A. F., Hespanha, J. P., Murray, R. M., & Hassibi, B. (2009). Data transmission over networks for estimation and control. *IEEE Transactions on Automatic Control*, *54*(8), 1807–1819. http://dx.doi.org/10.1109/TAC.2009.2024567.

Heemels, W. P. M. H., Teel, A. R., van de Wouw, N., & Nesic, D. (2010). Networked control systems with communication constraints: Tradeoffs between transmission intervals, delays and performance. *IEEE Transactions on Automatic Control*, *55*(8), 1781–1796. http://dx.doi.org/10.1109/TAC.2010.2042352.

Hu, Z., Shi, P., Zhang, J., & Deng, F. (2021). Control of discrete-time stochastic systems with packet loss by event-triggered approach. *IEEE Transactions on Systems, Man, and Cybernetics: Systems*, *51*(2), 755–764. http://dx.doi.org/10.1109/TSMC.2018.2882590.

IEC 62734 (2014). *Industrial networks—Wireless communication network and communication profiles—ISA 100.11a*. International Electrotechnical Commission.

Impicciatore, A., Tsiamis, A., Zacchia Lun, Y., D'Innocenzo, A., & Pappas, G. J. (2022). Secure state estimation over Markov wireless communication channels. In *2022 IEEE 61st Conference on Decision and Control (CDC)* (pp. 2935–2940). http://dx.doi.org/10.1109/CDC51059.2022.9992668.

Impicciatore, A., Zacchia Lun, Y., Pepe, P., & D'Innocenzo, A. (2024). Optimal output-feedback control over Markov wireless communication channels. *IEEE Transactions on Automatic Control*, *69*(3), 1643–1658. http://dx.doi.org/10.1109/TAC.2023.3328268.

Kawka, P. A., & Alleyne, A. G. (2006). Stability and performance of packet-based feedback control over a Markov channel. In *2006 American Control Conference* (pp. 2807–2812). IEEE, http://dx.doi.org/10.1109/ACC.2006.1656649.

Li, H., Han, C., Zhang, H., & Xie, L. (2021). Optimal control and stabilization for networked systems with input delay and Markovian packet losses. *IEEE Transactions on Systems, Man, and Cybernetics: Systems*, *51*(7), 4453–4465. http://dx.doi.org/10.1109/TSMC.2019.2938792.

Li, H., Li, X., & Zhang, H. (2021). Optimal control for discrete-time NCSs with input delay and Markovian packet losses: Hold-input case. *Automatica*, *132*, Article 109806. http://dx.doi.org/10.1016/j.automatica.2021.109806.

Liu, W., Nair, G., Li, Y., Nesic, D., Vucetic, B., & Poor, H. V. (2021). On the latency, rate, and reliability tradeoff in wireless networked control systems for IIoT. *IEEE Internet Things Journal*, *8*(2), 723–733. http://dx.doi.org/10.1109/JIOT.2020.3007070.

Liu, W., Quevedo, D. E., Li, Y., Johansson, K. H., & Vucetic, B. (2022). Remote state estimation with smart sensors over Markov fading channels. *IEEE Transactions on Automatic Control*, *67*(6), 2743–2757. http://dx.doi.org/10.1109/TAC.2021.3090741.

Lu, Z., Zhong, S., & Qu, L. (2018). A switching approach to packet loss compensation strategy. *IEEE Access*, *7*, 5609–5615. http://dx.doi.org/10.1109/ACCESS.2018.2888518.

Matei, I., Martins, N. C., & Baras, J. S. (2008). Optimal linear quadratic regulator for Markovian jump linear systems, in the presence of one time-step delayed mode observations. *IFAC Proceedings*, *41*(2), 8056–8061. http://dx.doi.org/10.3182/20080706-5-KR-1001.01360, 17th IFAC World Congress.

Minero, P., Coviello, L., & Franceschetti, M. (2013). Stabilization over Markov feedback channels: The general case. *IEEE Transactions on Automatic Control*, *58*(2), 349–362. http://dx.doi.org/10.1109/TAC.2012.2212616.

Mo, Y., Garone, E., & Sinopoli, B. (2013). LQG control with Markovian packet loss. In *2013 European Control Conference (ECC)* (pp. 2380–2385). IEEE, http://dx.doi.org/10.23919/ECC.2013.6669778.

Moayedi, M., Foo, Y. K., & Soh, Y. C. (2013). Networked LQG control over unreliable channels. *International Journal of Robust and Nonlinear Control*, *23*(2), 167–189. http://dx.doi.org/10.1002/rnc.1822.

Okano, K., & Ishii, H. (2017). Stabilization of uncertain systems using quantized and lossy observations and uncertain control inputs. *Automatica*, *81*, 261–269. http://dx.doi.org/10.1016/j.automatica.2017.03.036.

Pajic, M., Sundaram, S., Pappas, G. J., & Mangharam, R. (2011). The wireless control network: A new approach for control over networks. *IEEE Transactions on Automatic Control*, *56*(10), 2305–2318. http://dx.doi.org/10.1109/TAC.2011.2163864.

Park, P., Ergen, S. C., Fischione, C., Lu, C., & Johansson, K. H. (2018). Wireless network design for control systems: A survey. *IEEE Communications Surveys & Tutorials*, *20*(2), 978–1013. http://dx.doi.org/10.1109/COMST.2017.2780114.

Peters, E. G. W., Marelli, D., Quevedo, D. E., & Fu, M. (2019). Predictive control for networked systems affected by correlated packet loss. *International Journal of Robust and Nonlinear Control*, *29*(15), 5078–5094. http://dx.doi.org/10.1002/rnc.3896.

Pezzutto, M., Tramarin, F., Dey, S., & Schenato, L. (2020). Adaptive transmission rate for LQG control over Wi-Fi: A cross-layer approach. *Automatica*, *119*, Article 109092. http://dx.doi.org/10.1016/j.automatica.2020.109092.

Quevedo, D. E., Østergaard, J., & Ahlén, A. (2014). Power control and coding formulation for state estimation with wireless sensors. *IEEE Transactions on Control Systems Technology*, *22*(2), 413–427. http://dx.doi.org/10.1109/TCST.2013.2253464.

Sadeghi, P., Kennedy, R., Rapajic, P., & Shams, R. (2008). Finite-state Markov modeling of fading channels – A survey of principles and applications. *IEEE Signal Processing Magazine*, *25*(5), 57–80. http://dx.doi.org/10.1109/MSP.2008.926683.

Schenato, L., Sinopoli, B., Franceschetti, M., Poolla, K., & Sastry, S. S. (2007). Foundations of control and estimation over lossy networks. *Proceedings of the IEEE*, *95*(1), 163–187. http://dx.doi.org/10.1109/JPROC.2006.887306.

Seiler, P., & Sengupta, R. (2005). An H_∞ approach to networked control. *IEEE Transactions on Automatic Control*, *50*(3), 356–364. http://dx.doi.org/10.1109/TAC.2005.844177.

Wang, D., Wang, J.-l., & Wang, W. (2013). H_∞ controller design of networked control systems with Markov packet dropouts. *IEEE Transactions on Systems, Man, and Cybernetics: Systems*, *43*(3), 689–697. http://dx.doi.org/10.1109/TSMCA.2012.2211587.

Wu, J., & Chen, T. (2007). Design of networked control systems with packet dropouts. *IEEE Transactions on Automatic Control*, *52*(7), 1314–1319. http://dx.doi.org/10.1109/TAC.2007.900839.

Xie, L., & Xie, L. (2009). Stability analysis of networked sampled-data linear systems with Markovian packet losses. *IEEE Transactions on Automatic Control*, *54*(6), 1375–1381. http://dx.doi.org/10.1109/TAC.2009.2015558.

Xu, J., Gu, G., Tang, Y., & Qian, F. (2022). Channel modeling and LQG control in the presence of random delays and packet drops. *Automatica*, *135*, Article 109967. http://dx.doi.org/10.1016/j.automatica.2021.109967.

You, K., & Xie, L. (2010). Minimum data rate for mean square stabilizability of linear systems with Markovian packet losses. *IEEE Transactions on Automatic Control*, *56*(4), 772–785. http://dx.doi.org/10.1109/TAC.2010.2068590.

Yu, J., & Fu, L. C. (2015). An optimal compensation framework for linear quadratic Gaussian control over lossy networks. *IEEE Transactions on Automatic Control*, *60*(10), 2692–2697. http://dx.doi.org/10.1109/TAC.2015.2406977.

Zacchia Lun, Y., & D'Innocenzo, A. (2019). Stabilizability of Markov jump linear systems modeling wireless networked control scenarios. In *2019 IEEE 58th Conference on Decision and Control (CDC)* (pp. 5766–5772). IEEE, http://dx.doi.org/10.1109/CDC40024.2019.9029202.

Zacchia Lun, Y., D'Innocenzo, A., & Di Benedetto, M. D. (2019). Robust stability of polytopic time-inhomogeneous Markov jump linear systems. *Automatica*, *105*, 286–297. http://dx.doi.org/10.1016/j.automatica.2019.03.031.

Zacchia Lun, Y., Rinaldi, C., Alrish, A., D'Innocenzo, A., & Santucci, F. (2020). On the impact of accurate radio link modeling on the performance of WirelessHART control networks. In *2020 IEEE Conference on Computer Communications (INFOCOM)* (pp. 2430–2439). IEEE, http://dx.doi.org/10.1109/INFOCOM41043.2020.9155285.

Zacchia Lun, Y., Rinaldi, C., D'Innocenzo, A., & Santucci, F. (2024). Co-designing wireless networked control systems on IEEE 802.15.4-based links under Wi-Fi interference. *IEEE Access*, *12*, 71157–71183. http://dx.doi.org/10.1109/ACCESS.2024.3402082.

Zacchia Lun, Y., Smarra, F., & D'Innocenzo, A. (2025). Optimal control over Markovian wireless communication channels under generalized packet dropout compensation—extended version. https://arxiv.org/abs/2501.17105.

Yuriy Zacchia Lun is an Assistant Professor in the Department of Information Engineering, Computer Science, and Mathematics at the University of L'Aquila. He received an MS degree in telecommunications engineering from the University of L'Aquila in 2012 and a joint Ph.D. degree in computer science from the Gran Sasso Science Institute (GSSI), L'Aquila, and the IMT School for Advanced Studies Lucca, Lucca, Italy, in 2017. In 2017, he was a Visiting Ph.D. Student in ERASMUS+ Traineeship with the Department of Computer Science, University of Oxford, UK. He was a Research Collaborator with the University of L'Aquila and the Center of Excellence DEWS from 2017 to 2018 and the IMT School for Advanced Studies Lucca from 2018 to 2022. His research interests include co-designing communication, computation, and control, formal methods, stochastic hybrid systems, wireless networked control systems, and cyber–physical system security.

Francesco Smarra is currently a Researcher at the University of L'Aquila, where he also received an MS degree in control and systems engineering and a Ph.D. degree in Electrical and Information Engineering, respectively, in 2010 and 2014. He has held visiting scholar positions at UC Berkeley (2012–2013) and the University of Pennsylvania (2014–2015) and research positions at the University of Pennsylvania (2016–2017). He was the recipient of the Best Application Paper Award of the European Control Conference in 2015. He obtained the National Scientific Qualification for the role of Associate Professor in Control Theory. His research interests are in control theory, modeling and control of complex systems via machine learning, wireless networked control systems, building automation systems, and structural health monitoring systems.

Alessandro D'Innocenzo is an Associate Professor in the Department of Information Engineering, Computer Science, and Mathematics at the University of L'Aquila. In 2007, he obtained a Ph.D. degree in Electrical and Information Engineering from the University of L'Aquila and accomplished the International Curriculum Option of Doctoral Studies in Hybrid Control for Complex, Distributed, and Heterogeneous Embedded Systems. In 2007 and 2009, he was a Postdoctoral Researcher in the Department of Electrical and Information Engineering of the University of L'Aquila. In 2008, he was a Postdoctoral Researcher in the Department of Electrical and Systems Engineering of the University of Pennsylvania. In 2005, he was the recipient of the Fondazione Filauro award for Ph.D. students, and in 2015, of the Best Application Paper Award of the European Control Conference. In 2019, he obtained the National Scientific Qualification for the role of "Professore di I fascia" (Professor) in Control Theory. He is a coordinator of several EU-funded research projects, a member of the Executive Committee of the Centre of Excellence EX-Emerge, a delegate for the University of L'Aquila in the "Fondazione ITS Academy Abruzzo," and co-founder of the Academic Spin-off "Nindo Srl." He is currently Head of the bachelor's degree in information engineering at the University of L'Aquila. His research focuses on integrating control theory and machine learning algorithms with applications to automation and communication networks.